MODELLING OF COLUMNS AND FIBRE REINFORCED LOAD TRANSFER PLATFORM SUPPORTED EMBANKMENTS

Liet Chi Dang[1], Cong Chi Dang[2], and Hadi Khabbaz[3]

[1]Ph.D. Candidate, School of Civil and Environmental Engineering, University of Technology Sydney, Ultimo, NSW 2007, Australia, liet.dang@uts.edu.au

[2]Senior Civil Engineer, Hau Giang Department of Environment and Natural Resources, Hau Giang Province, 910000, Viet Nam, chicongct1912@gmail.com

[3]Associate Professor, School of Civil and Environmental Engineering, University of Technology Sydney, Ultimo, NSW 2007, Australia, hadi.khabbaz@uts.edu.au

ABSTRACT: This study proposes a novel ground modification technique utilising fibre reinforced load transfer platform (FRLTP) and deep cement mixing (DCM) columns supported (CS) embankment constructed over soft soils. An equivalent two-dimensional finite element model was developed to simulate the full geometry of a CS embankment reinforced without or with an FRLTP. A series of numerical analyses was firstly conducted on the proposed model for different improvement depths to assess the effectiveness of the introduction of FRLTP into the CS embankment system in terms of total and differential settlements, stress transfer mechanism and lateral displacement with depth. Subsequently, another extensive parametric study was conducted to further investigate the influence of the FRLTP key parameters including elastic deformation modulus, shear strength properties, and tensile strength on the embankment performance during construction and consolidation time. The numerical results show that the embankment with FRLTP can effectively diminish the total settlement and the lateral deformation of the embankment, meanwhile improve the stress concentration ratio and the embankment stability to a great extent. The findings of the extensive parametric study indicate that the FRLTP shear strength properties appear to be the most influence factors to be considered in the design procedure of a target CS-FRLTP-embankment system.

1. INTRODUCTION

The fast development of essential infrastructure including roads and rail networks, being constructed in many countries worldwide, is to meet the demand of the dramatic increase in population and economic growth. As a result, many countries are experiencing the lack of readily available stiff grounds in support to such transport infrastructure projects. Thus, many road and highway

embankments have to be founded on soft grounds. This practice is highly risky, because soft ground has a low bearing capacity, insufficient shear strength and high compressibility. Therefore, to ensure the stability of embankment during the construction process and its long-term service life, appropriate ground improvement techniques are needed to be adopted in enhancing the engineering properties of soft soil or even for transferring embankment and traffic loads to a deeper and stiffer soil stratum.

A growing number of ground modification approaches have been applied to improve soft soil properties to support embankment construction such as:

- Preloading with the vertical drain application (Liu & Rowe 2015; Parsa-Pajouh et al. 2015)
- Excavating the existing soft ground and substituting it with high shear strength and bearing capacity backfill soil
- Reducing embankment load using lightweight fill materials (Dang 2018; Dang et al. 2015; Dang & Khabbaz 2018a; Dang et al. 2018c; Martin et al. 1990)
- Constructing in stages and leaving time for consolidation
- Improving soft ground underneath embankment by chemical treatment (Chai et al. 2015; Dang et al. 2016b; Dang et al. 2016c; Dang & Khabbaz 2018b, 2018c, 2019; Dang et al. 2017b, 2017c; Fatahi & Khabbaz 2013, 2015; Jamsawang et al. 2016)
- Stone columns (Fatahi et al. 2012)
- Geosynthetic-reinforced and piles supported earth platform (Dang et al. 2016a; Han & Gabr 2002; Liu et al. 2007).

On top of those methods, the ground improvement technique using deep cement mixing columns has widely been used in construction practice. Of the main reasons is that it provides an economical and fast ground improvement solution for the construction of road and highway embankments over soft soil (Chai et al. 2015; Venda Oliveira et al. 2011; Yapage et al. 2014; Yapage et al. 2015). In order to improve the soft soil characteristics such as bearing capacity, shear strength and compressibility, in wet mixing method, slurry cement is mixed with soft ground at a designated water/cement ratio during the DCM columns construction process, while dry cement is mixed with in-situ soils to establish artificial DCM columns in dry mixing method. However, most of road and railway embankments built on end bearing piles/columns are most likely to be subjected to large differential settlements between the embankment and the adjacent roads due to the different stiffness levels (Chai et al. 2015; Liu & Rowe 2015). It is known that floating soil columns provide a less stiff ground foundation, but they are more cost-effective and technically feasible than the end bearing

columns, when soft foundation soils reach greater depth. Furthermore, one advantage of the floating columns solution is that when a sand layer acting like an aquifer layer directly located below soft ground layers, the soft ground improvement solution using floating DCM columns could be the best choice for not contaminating groundwater during construction and post-construction. The experimental investigation by Chen & Indraratna (2014) also indicated that conventional chemical stabilisers (e.g. lime, cement) for soil stabilisation might cause adverse effects on the environment by changing the pH level of treated soil and its surrounding areas. As a result, the quality of groundwater and the normal growth of vegetation can be affected because of the pH change. As such, Chai et al. (2015) reported that using the floating DCM columns could be the best solution for soft ground improvement because it would leave an intact clay sub-layer below the column tip and immediately above the aquifer. As expected, such soft clay sublayer would serve as a barrier to hindering hazardous chemicals from spreading out of the deep cement mixing soil improvement area into groundwater. Nevertheless, the analysis and design of floating soil columns are complex, involve considering complicated soil-structure interaction, and there are no specific standards and guidelines readily available for the design of embankments supported on floating cement-soil columns.

Numerical modelling based on the finite element method (FEM) has been used as an effective tool in predicting the performance of DCM columns supported embankments founded on soft ground in terms of the total and differential settlements, the horizontal movement, the rate of settlement, the slope stability and the degree of consolidation over a long period of time. The finite element numerical modelling can reasonably simulate the load transfer mechanism between DCM columns and foundation soil, and the generation and dissipation of excess pore water pressures. Consequently, the numerical modelling assist in predicting the total settlement, the lateral displacement, the bending moment of DCM columns with depth under the embankment using three-dimensional FEM model or even with an equivalent two-dimensional (2D) plane strain FEM model (Chai et al. 2015; Dang et al. 2016a; Tan et al. 2008; Yapage et al. 2014). Nevertheless, most of the numerical investigations have been recently performed to investigate the behaviour of embankments over DCM columns (Chai et al. 2015; Yapage et al. 2014), the performance of geosynthetic reinforced traditional angular layer as a load transfer platform (LTP) and piles/columns supported embankments over soft soils (Han & Gabr 2002; Liu et al. 2007; Yapage et al. 2015). According to Zhang et al. (2013), the popular applications of the geosynthetic reinforced traditional angular platform over columns supported embankments built on top of soft soils have come up with many geotechnical difficulties, namely intolerable total and differential settlements, larger lateral earth pressure and displacement, local or

global instability, and potential failures due to over-bearing or bending capacity of DCM columns. Therefore, a novel ground modification technique utilising eco-friendly, low cost and recycled materials such as lime-soil-fibre reinforced load transfer platform (FRLTP) to be used as a replacement of geosynthetic reinforced traditional angular platform layer combined with DCM columns supported embankments constructed on top of multilayers of soft soils is required to overcome those aforementioned geotechnical difficulties.

Previous studies conducted by Consoli et al. (2009b) show that fibre reinforcement of cement treated soils in engineering practices has been proven very effective in improving the peak and post-peak shear strengths and the bearing capacity of soil foundations, while reducing the initial stiffness and transforming the brittle behaviour of cemented soils to become more ductile material. Furthermore, Consoli et al. (2009a) conducted another experimental program on the effect of relative density on the plate loading test on fibre reinforced sand; and reported that the load-settlement behaviour was significantly affected by the relative density and the fibre inclusion. Specifically, the inclusion of fibres increased the overall strength, stiffness and bearing capacity of sandy soils by a mechanism called the partial suppression of dilation and interaction among sand grains and fibres. Meanwhile, an increase in the relative density significantly reduced the settlement of reinforced soils, when compared to non-reinforced soils. From the experimental results, they also observed that the fibre reinforced sand could be useful for embankments over soft soils because it had high potential to maintain its strength when undergoing large total and differential settlements, and changing to be a very ductile material.

Tang et al. (2007) investigated the strength and mechanical behaviour of short fibre reinforced cemented soils and also confirmed that the improvement of the compressive and shear strength, the axial strain at failure. They found the ductility of clayed soils reinforced with fibre inclusion was greater for a higher soil density. A review of soil reinforcement using randomly distributed fibres by Wang et al. (2017) indicated that adding such type of fibre reinforcement of soils effectively increases the engineering characteristics of reinforced soils. They include an increase in the shear and compressive strengths, California bearing capacity, wetting and drying cycles, freezing-thawing behaviour, shrinkage and swelling behaviour, ductility (or brittleness reduction), resistance to liquefaction and desiccation cracking. In addition, Wang et al. (2017) reported that as compared to traditional geosynthetic reinforcement, which is normally placed in soils by different layers with a predetermined orientation, the addition of randomly distributed fibres into soils is more effective in maintaining the isotropic soil strength without presenting the potential of weak planes, which tend to develop along with the interfaces between soil and the geosynthetic layer. Therefore, employing fibre

reinforcement of soils has increasingly become an extensive research interest in recent years in order to examine its application in various construction practices such as load transfer platform supported embankments.

In recent years, Okyay & Dias (2010) investigated the mechanical characteristics of lime/cement stabilised soils used as an LTP using numerical analysis of a unit cell model, considering the influences of pile spacing, shear strength, stiffness and the height of stabilised soil platform. The results of their numerical analysis revealed that the efficacy of the stabilised soil platform was significantly affected by the shear strength parameters; meanwhile the effect of LTP stiffness reduced with increasing the embankment loading. It is worth mentioning that the numerical investigation of Okyay & Dias (2010) was mainly based on a two-dimensional axisymmetric unit cell model. Hence, it was unable to fully capture the effects of stabilised soils as an LTP on the actual stress transfer mechanism between columns in a group and surrounding soil, the differential settlements and the lateral movement in comparison with the full geometry model of embankment (Yapage & Liyanapathirana 2014). Based on a numerical modelling reported by Okyay & Dias (2010), Anggraini et al. (2015) studied the performance of a lime-fibre reinforced soil platform and rigid piles supported embankment over soft soil by both physical and numerical modelling using a 2D axisymmetric unit cell model. From the numerical results, they reported that the application of the lime-fibre reinforced soil platform was very effective in reducing the differential settlement, while relatively enhancing the efficacy and the bending performance of the reinforced soil platform. They also explained that thickness, the tensile stiffness, the shear strength properties of the reinforced soils platform had significant influences on the differential settlement and the efficacy of the embankment. Nonetheless, as a 2D unit cell model scaled down was adopted in their study, the influences of the lime-fibre reinforced LTP and the group effect of rigid pile interactions on the lateral deformation, the soil arching effect, the variations of excess pore water pressure were crucial but not taken into account in the physical and numerical modeling. Due to the above mentioned limitations, the efficacy of the lime-fibre reinforced LTP and piles supported embankment system investigated by Anggraini et al. (2015) was relatively small (approximately 30%) as compared to the reported efficacy of the lime/cement stabilised LTP supported embankment with piles numerically analysed by Okyay & Dias (2010). Nguyen et al. (2016) conducted 2D numerical investigations on the failure pattern of columns supported embankment with cement stabilised slab as an LTP by taking the effect of the cement stabilised slab on the failure pattern of DCM columns. The results of finite element analysis revealed that the stabilised LTP thickness and compressive strength exhibited notable influence on the embankment horizontal displacement. Nguyen et al. (2016) reported that the influences of the

stabilised LTP on the embankment lateral displacement and the yield stress of columns subjected to the embankment load were greater for the higher compressive strength regardless of the LTP thickness. Dang et al. (2016a) conducted a two-dimensional numerical assessment of FRLTP as a likely replacement of geosynthetics reinforced traditional angular LTP in combination with piles supported highway embankments founded on soft grounds. By comparing the predicted result of numerical simulations with both the measured and predicted results, well reported in the literature, they concluded that the combined use of FRLTP and piles supported embankments experienced similar engineering characteristics compared to the geosynthetics reinforced traditional angular LTP supported embankment with piles. However, none of those investigations fully considered the influence of the lime/cement-fibre reinforced LTP (stabilised slab or mat) engineering properties on the performance of columns/piles supported embankments using a full geometry embankment model. As such, investigating the mechanical behaviour (e.g. the stress concentration ratio between columns within a group and surrounding soil with the embankment loading, the differential settlements, and the lateral displacement with depth) of columns supported embankment with a lime-fibre stabilised slab is crucial to be comprehensively considered based on the full geometry embankment model.

In this paper, a novel ground modification technique utilising FRLTP (fibre reinforced load transfer platform) and DCM columns supported embankment constructed on top of multilayers of soft soils is proposed and investigated based on the finite element method incorporated in PLAXIS. Numerical simulations using an equivalent 2D FEM model with proper modified parameters of structure and soil models have been adopted to examine the behaviour of floating DCM columns supported embankment without or with FRLTP built over soft soils. Firstly, a series of numerical analyses was carried out on the full geometry of DCM columns supported (CS) embankment reinforced without or with an FRLTP for various improvement depths of soft soils in a two-dimensional plane strain condition to investigate the effectiveness of adding FRLTP into the CS embankment system. Several embankment design parameters such as maximum and differential settlements, lateral displacement, load transfer mechanism between columns and foundation soils were analysed and examined. Subsequently, another extensive parametric study on the influential factors such as the FRLTP elastic deformation modulus (Young's modulus), the shear strength parameters and the tensile strength of the FRLTP, has been conducted to comprehend the performance of the floating DCM columns combined with FRLTP supported embankment. Based on the numerical findings, comparisons and comprehensive discussion on the variations of the total and differential settlement, the stress transfer mechanism between DCM columns and foundation soils with the embankment height, and the lateral displacement with depth, were undertaken to have a further

understanding of the embankment behaviour with FRLTP inclusion. The most influential factors of the FRLTP properties on the performance of the floating DCM columns embankment system are also highlighted and discussed in detail, which aim to enhance the design code for the floating DCM columns and FRLTP supported embankment found on multilayered soft soils.

2. CASE STUDY

Another hypothetical construction of natural fibre-reinforced load transfer platform and DCM columns supported highway embankment over soft clay layers is considered in this numerical investigation. The embankment geometry is shown in Figure 1 representing the only right half of the domain of the embankment since the embankment is symmetrical along its centreline. As can be seen from Figure 1, the embankment is 20.8 m wide and 6 m high with a 1V:1.8H side slope. The embankment is made of good quality soil with a cohesion of 20 kPa, a friction angle of 35° and an average unit weight of 19 kN/m^3. It is constructed on a 1 m thick fill material as a surface layer overlaying an 11 m thick deposit of soft clay. This deposit of soft clay overlies a 3 m thick stiff clay stratum followed by a 15 m thick sand layer. It should be noted that the stiff clay and sand layers were selected in this case study, as an attempt to simulate typical subsoil conditions in the field below embankments reported by many researchers (Chai et al. 2015; Chai et al. 2017). The ground-water table is located at a depth of 1 m below the ground surface. Details of these soil layers are summarised in Table 1. A fibre-lime-soil layer of 0.5 m is adopted in this numerical modelling and serves as an FRLTP, placed on the top of DCM columns improved soft soils.

To improve the engineering properties such as bearing capacity, shear strength, and compressibility of the thick soft soil strata of 12 m, deep cement mixing columns with 1.2 m diameter and 10 m length are used, which yield an improvement depth ratio (β) of roughly 83%. It can be noted that the improvement depth ratio (β) is defined as the depth of the DCM columns to the depth of soft soils from the embankment base to the top of a stiffer soil layer, which is the stiff clay in this numerical analysis. β=0 implies that soft soils are not improved with DCM columns, whereas β=1 means that soft soils are fully improved with DCM columns. With the improvement depth ratio of β=0.83 chosen in this case, the DCM columns are considered as floating columns supported embankment. In addition, the DCM columns are arranged in a square grid pattern with a centre-to-centre spacing of 1.9 m, which results in an area replacement ratio (α) of approximately 31% corresponding to those aforementioned geometric properties. It is noted that for a hypothetical embankment modelling, the DCM column parameters were selected to represent the typical soil-cement column properties from

published data available in the literature. Therefore, the unconfined compressive strength ($q_{u)}$ was assumed to be 1000 kPa (Chai et al. 2015) and the 100 MPa young modulus (E) of DCM columns was determined using the correlation $E=100q_u$ (Yapage et al. 2014). The 150 kPa tensile strength of the DCM columns was considered to $0.15q_u$ (CDIT 2002; Jamsawang et al. 2016) and the undrained shear strength of 500 kPa of DCM columns was assumed to be $s_u=1/2q_u$ (Filz & Navin 2006). The average unit weight of 15 kN/m^3 was considered to be in a range of 3%-15% higher than that of soft soils (CDIT 2002) and a Poisson's ratio of 0.15 (Chai et al. 2015) was selected as of the typical properties of DCM columns.

The construction sequence of the embankment is assumed to be in 0.5-1 m lifts at an average filling rate of 0.06 m/day to a total height of 6 m including the FRLTP with a height of 0.5 m. Following the completion of embankment construction, the consolidation period is left for 2 years. Table 2 shows the simulated construction sequence of the highway embankment used in this numerical modelling.

3. NUMERICAL MODELLING

3.1. Finite element models and parameters

A two-dimensional plane strain model was built using commercial finite element software PLAXIS 2D, adopting the equivalent 2D numerical analysis method proposed by previous researchers (Chai et al. 2015; Dang et al. 2016a; Dang et al. 2017a; Okyay & Dias 2010; Tan et al. 2008) to simulate the performance of FRLTP and DCM columns supported highway embankment. The equivalent 2D model was selected because of less analysis time consuming, while generating results with reasonable accuracy. For instance, it was reported that the settlement results predicted by 2D modelling were up to 9% (Tan et al. 2008), around 10% (Chai et al. 2015), and roughly 15% (Ariyarathne et al. 2013), different with the corresponding predictions using 3D modelling. The DCM columns were simulated by continuous plane strain walls of 0.60 m thickness for the entire columns length of 10 m to maintain the same area of replacement ratio of approximately 31%, taking into account of the equivalent normal stiffness (EA) as implemented and recommended for numerical simulations of columns supported embankments by many researchers (Chai et al. 2015; Dang et al. 2018a; Yapage et al. 2015). Meanwhile, the centre to centre spacing between two adjacent walls in this numerical simulation was remained the same as the 1.9 m centre to centre spacing between two adjacent DCM columns.

Regarding the constitutive modelling, the DCM columns were modeled as a linear elastic-perfectly plastic material using Mohr-Coulomb (MC) model (Huang & Han 2010; Liu & Rowe 2015).

Similarly, the FRLTP, embankment and fill material were simulated using a linear elastic-perfectly plastic model with Mohr-Coulomb failure criterion. The Mohr-Coulomb material model requires Young's modulus (E), Poisson's ratio (ν), the effective cohesion (c'), the angle of internal friction (φ'), the dilation angle (ψ) and the tensile strength. Subsequently, the soft soil layers were represented by Modified Cam Clay (MCC) model. The required parameters for the MCC model are slope of the virgin consolidation line (λ), the slope of swelling line (κ), the initial void ratio (e_0), the slope of the critical state line (M), and Poisson's ratio (ν). It is assumed that the values of horizontal permeability (k_h) are about 1.5 times the corresponding values of vertical permeability (k_v) of the subgrade soils, whereas the horizontal and vertical permeability of sand and DCM columns are equal. A summary of the constitutive model parameters is presented in Table 1. During consolidation process due to an increase in embankment load, the hydraulic permeability was changed attributable to the relationship between the void ratio change and the corresponding embankment load; therefore, the permeable change index $C_k = 0.5e_0$ was adopted in this investigation.

Referring to Figure 2, only right half of the embankment is represented in this numerical simulation, since the embankment is symmetrical along its centreline. The foundation soil was taken to 30 m depth from the ground surface overlying a stiff clay stratum. The horizontal length of the FEM model was taken to be 80 m, which was almost three times the half width of the embankment base, in order to minimise the boundary effect. Both the left and right boundaries were considered to be impermeable, meanwhile pore fluid flow was permitted from both the ground surface and the bottom boundaries.

In this analysis, for the 2D plane strain FEM model, the horizontal displacement at the left and right boundaries was not permitted, but the vertical movement was allowed, whereas both the vertical and horizontal displacements were prevented at the bottom boundary. On one hand, due to the relatively high permeability, the embankment fill and sand stratum were assumed to behave in a drained condition. On the other hand, FRLTP, DCM columns, and other four foundation soils were assumed to act as undrained material. In this modelling, fifteen-node triangular elements with excess pore water pressure degrees of freedom at all nodes were adopted to simulate the foundation soils, DCM columns and FRLTP, while fifteen nodes triangular elements without excess pore water pressure degrees of freedom at all nodes were applied to model the embankment fill and sand layers.

3.2. Model validation

Prior to this numerical modelling, a case study of DCM columns supported highway embankment without reinforcement of load transfer platform reported by Chai et al. (2015) was used to validate the proposed modelling approach of a CS embankment investigated in this numerical simulation working reasonably. Through the field measurements and numerical predictions, Chai et al. (2015) reported very well the results of settlements with time at column head and foundation soil between two DCM columns under the centre of the CS highway embankment base. The detailed simulation procedure for the embankment analysis can be found in Chai et al. (2015). In this simulation, settlements between this predicted results and those measured and predicted outcomes by Chai et al. (2015) related to the ground surface settlement and the column settlement on top at the centreline of the embankment base during embankment construction and consolidation periods up to 559 days are presented in Figure 3 and then a related thorough comparison was made. Observation of the predicted and measured settlements illustrated in Figure 3 notes that the development of the predicted settlements with time derived from this equivalent 2D finite element modelling of a CS embankment shows good agreement with those measured settlements reported by Chai et al. (2015). Meanwhile, the 3D prediction by Chai et al. (2015) underestimated the settlements at both the column top and the ground surface between two adjacent columns as shown in Figure 3a and 3b. According to Chai et al. (2015), the influences of 3D simulation could produce the faster load reduction with depth as compared to 2D simulation and the higher order displacement shape function used for elements in the 2D analysis as compared to 3D analysis by PLAXIS could be possible reasons for the underestimated settlements by the 3D prediction. In general, the predicted results reveal that the equivalent 2D FEM model proposed in this numerical analysis is suitable for simulating the behaviour of DCM columns supported embankment built on multilayers of soft soils.

4. RESULTS AND DISCUSSION

4.1. Effect of the different improvement depths on the embankment behaviour

4.1.1. Variation of total and differential settlements for different improvement depths

Figure 4a displays the development of the ground surface settlement versus elapsed time between two adjacent DCM columns under the centre of the embankment without or with FRLTP for different improvement depth ratios (β). It can be noted that the improvement depth ratio (β) is defined as the ratio of DCM column length to soft soil thickness. To investigate the effect of floating DCM columns on the total and differential settlements of embankment, the columns length was varied from β=0.5

to β=1. As plotted in Figure 4a, the time-dependent surface settlement increased significantly during the first period of 100 days due to the increase in embankment load. This phenomenon was followed by a gradual increase in the surface settlement up to two years after the completion of the embankment construction owing to the evolution of consolidation with time. Moreover, the significant reduction of surface settlement with increasing the improvement depth ratio from β=0.5 to β=1 was clearly observed in Figure 4a. To be more specific, the significant surface settlement of approximately 1.47 m as numerically predicted for the improvement depth ratio of β=0.5 decreased to a relatively small value of 0.35 m with the increase of β value up to 1 (for the end-bearing columns). The predicted settlement results also reveal that the increase in DCM columns length not only decreased the final surface settlement but also resulted in the improvement of consolidation process of soft soil strata. For example, the surface settlement in case of the end-bearing columns (β=1) reached its final settlement after approximately 200 days of elapsed time, whereas the final surface settlement in case of the floating DCM columns (β=0.5) was not reached after the 830 days of investigation period, displaying a trend of continuous settlement.

It is also important to note that the surface settlement in the case of floating DCM columns (β=0.83) supported embankment without or with FRLTP was visually depicted in Figure 4a for evaluation of the effect of FRLTP inclusion on the total settlement of the entirely DCM columns-embankment system. It can apparently be seen from this figure that the surface settlement of the embankment without FRLTP was definitely larger than that of the embankment with FRLTP, which can clearly be observed throughout the 830 days of investigation period. The maximum settlement of the embankments with FRLTP at the end of the 2 years consolidation period was about 0.64 m, which was relatively smaller than the 0.77 m settlement of the embankment without FRLTP. This numerical finding indicates that the effectiveness of FRLTP inclusion in minimising the final surface settlement of the entire DCM columns-embankment system.

The effect of different improvement depth ratios (β) on the total settlement at the embankment base centre is shown in Figure 4b. It is observed that the total settlement significantly and linearly decreased by approximately 76% for the post-construction of embankment case as the improvement depth ratio increased. Figure 4b also shows that the consolidation time has a great influence on the changes in the maximum total settlement of the embankment with FRLTP when the improvement depth ratio (β) increases from 0.5 to 1. Approximately 60% difference in the maximum total settlement between the construction completion and the 2 years post-construction can be observed in Figure 4b when the column length is short (β=0.5), but it becomes smaller and approaches a

comparable value when the column length increases to 12 m (β=1). The improvement in the time-dependent total settlement when the improvement depth ratio increased could be due to an increase in the columns length approaching to a stiffer layer. As expected, in this condition, most of the embankment load transfers to the stiffer clay soil. Therefore, the effects of the time-dependent settlement of the underlying soft soils due to the embankment load become negligible.

The variation of differential settlement under the centre of the embankment base without or with FRLTP inclusion along with embankment height for different improvement depth ratios (β) can be observed in Figure 5. Similar to the trend of surface settlement of the embankment with FRLTP, the differential settlement on the ground surface, defined as the settlement difference between the top of DCM columns (see point A in Figure 1) and the ground surface between two adjacent DCM columns (see point B in Figure 1), increased with an increase in the embankment height, whereas decreased with increasing the improvement depth ratio (β) from 0.5 to 1. By comparing with embankment with FRLTP for the same improvement depth ratio (β=0.83), the increase in differential settlement with the embankment height was more noticeable for the embankment without FRLTP as presented in Figure 5. On one hand, the differential settlement of the embankment without FRLTP linearly increased with embankment height from 0.5 m to 6 m, which resulted in the accumulated differential settlement of approximately 125 mm at the end of embankment construction. On the other hand, as evident in Figure 5, the differential settlement of the embankment with FRLTP showed a nonlinear increase with increasing the embankment height and it seemly started to appear when embankment height increased from only 3 m to 6 m. The accumulated differential settlement of the embankment with FRLTP was about 33 mm at the end of embankment construction, which led to about 73% reduction of the differential settlement compared with that of the embankment without FRLTP. Furthermore, in the cases of the embankment with FRLTP for different improvement depths, a significant reduction of the maximum differential settlement was observed in a wide range between 52% and 80% in comparison with that of the embankment without FRLTP when the β value increased from 0.5 to 1. It can be concluded that the FRLTP inclusion showed a significant improvement in reducing the differential settlement of the DCM columns–embankment system. The improvement in the differential settlement could be attributed to the enhancement of soil arching effect above the top of DCM columns facilitated by the FRLTP inclusion as visibly illustrated in Figure 6.

4.1.2. Load transfer mechanism between columns and foundation soil for different improvement depths

Han & Gabr (2002) used the load transfer mechanism proposed by Terzaghi (1943) to examine the proportion of the embankment load transfer between columns and surrounding foundation soil, taking into consideration of the soil arching effect. According to Terzaghi (1943), with an increase in embankment fill causing embankment load increase, the embankment fill between columns tends to move downward due to the presence of soft foundation soil. The fill movement is partially resisted by its shear strength above the columns. Such shear strength resistance reduces the load from embankment to be transferred to soft foundation soil but increases the embankment load imposed on columns via the soil arching effect. The ratio of soil arching effect in embankment fill is defined in Equation (1) proposed by Terzaghi (1943) as follows:

$$\rho = \frac{P_b}{\gamma H + q} \tag{1}$$

where ρ is the soil arching ratio; ρ=0 implies the complete soil arching, whereas ρ=1 means no soil arching; P_b represents the amount of earth pressure on the surface of foundation soil between columns; γ represents the unit weight of embankment fill; H is the height of embankment; and q represents the uniform surcharge on the embankment if applicable.

According to Liu et al. (2007), the soil arching effect in embankment results in more of the embankment load transfer to columns from soft foundation soil. The load transfer between columns and surrounding soil can be estimated by a stress concentration ratio (SCR) defined in Equation (2) as the ratio of vertical effective stress on the DCM columns head (σ_c) to vertical effective stress applied to foundation soil (σ_s) between two adjacent DCM columns.

$$\text{SCR} = \frac{\sigma_c}{\sigma_s} \tag{2}$$

Figure 7 depicts the fluctuation of the stress concentration ratio on the DCM column head at the embankment centre in association with an increase in the embankment height for different improvement depth ratios (β). As illustrated in Figure 7, the SCR generally increased as the embankment height increased to a certain high value and then it decreased with higher increase in the embankment height in the cases of the embankment with FRLTP for different β values. Except for the embankment without FRLTP, that showed a minor increase in the SCR with further increase in

the embankment height up to 6 m. For example, the SCR value of the embankment without FRLTP significantly increased from approximately 2.5 to 12.5 with a relatively small increase in the embankment height from 0.5 m to 2 m. This was followed by a slight increase from 12.5 to a certain value of 14.7 with further increase in the embankment height up to 6 m. However, for the embankment reinforced with an FRLTP as plotted in Figure 7, the increase in embankment height from 0.5 m to 4 m resulted in the substantial increase in the SCR value ranging from approximately 5 to reach a peak between 57 and 100 for the improvement depth ratio (β) between 0.5 and 1, respectively. As observed in Figure 7, the additional increase in the embankment height up to 6 m gave rise to the corresponding decrease in the SCR value to a certainly high level between 20 and 58.

In comparison with the embankment without FRLTP, the peak SCR value of the embankment with FRLTP was about 3.9-7.2 times greater as the β value increased between 0.5 and 1. A significant improvement in SCR (or the increase in the soil arching effect) of the embankment with FRLTP to a certain height of the embankment, regardless of the improvement depth ratios (β), was considered as a direct consequence of reduction of the embankment load transfer to the foundation soil facilitated by the FRLTP inclusion. The high shear strength of lime-fibre reinforced load transfer platform contributed to the effective improvement in the SCR as recently reported by researchers (Dang et al. 2016a; Okyay & Dias 2010). However, further increase in the embankment height resulted in a decrease in the SCR value after reaching a peak, which might be due to the over bearing capacity of the DCM columns. In that circumstance, the additional increase in the embankment height would decrease the arching effect of the embankment, resulting in more load transferred to the foundation soil between columns. Thus, a decrease in the SCR value seems to signal the start of an increase in the differential settlement of the DCM columns supported embankment, as supporting evidence can be found in Figure 5 and 7.

4.1.3. Variation of lateral displacement with depth for different improvement depths

Figure 8a and 8b display the lateral displacement with depth of the DCM column under the embankment toe. It can obviously be seen from these figures that the lateral displacement decreased with an increase in the improvement depth ratio (β) from 0.5 to 1 regardless of the construction end or the 2 years post-construction. However, as observed in Figure 8a and 8b, the lateral displacement of DCM column tip increased significantly during the 2 year consolidation period, except for the case of the high improvement depth ratio between β=0.83 and β=1 for the end-bearing columns showing that the lateral displacement at 2 years post-construction remained almost constant. The increase in

the lateral displacement is primarily resulted from an increase in the height of the embankment fill that induces lateral spreading forces and lateral earth pressures acting on the DCM columns. An excessive increase in the lateral deformation can cause sliding, bending and tensile failure of the embankment. Thus, it is essential to prevent the excessive lateral deformation causing such aforementioned types of failure of the CS embankment by properly determining an optimum improvement depth ratio. In this investigation, the short floating DCM columns with β=0.5-0.7 revealed the remarkable lateral displacement at both ends of the DCM column, especially in the column tip. Hence, it could be unacceptable for the CS embankment design in terms of stability. However, as illustrated in Figure 9, with increasing the improvement depth ratio to β=0.7 or beyond, the lateral displacement decreased significantly and could be accepted. This is consistent with the early research (Jamsawang et al. 2016) reporting that the improvement depth ratio of β=0.7 might be an optimal value, required for the stability of a floating DCM columns-supported embankment over soft soils. The improvement of the lateral deformation along with the increase in the columns length could be attributed to approaching the fixity condition of the DCM columns into the stiffer layer below. In other words, the longer columns facilitate the better-restrained condition in support of the embankment loading and consequently minimise the lateral displacement.

In addition, the lateral movement of the DCM column under the toe of the embankment without or with FRLTP was depicted in Figure 8a and 8b for the completion of the embankment construction and the 2 years post-construction cases, respectively, for comparison purposes. As observed in Figure 8a and 8b, the introduction of the FRLTP into the CS embankment system reduced significantly the lateral movement of the column head compared to that of the embankment without FRLTP for the same improvement depth ratio of β=0.83. This improvement reconfirms that the FRLTP inclusion is highly effective in alleviating the lateral movement of the embankment, resulting in the enhancement of the embankment stability. The improvement in the lateral displacement of the embankment with FRLTP could be due to the high shear strength and tensile strength contributed from the lime-fibre reinforced platform.

4.2. Effect of the FRLTP elastic deformation modulus (Young's modulus, E) on the embankment behaviour

To investigate the effect of the elastic deformation modulus (stiffness) of FRLTP on the performance of the embankment with the same platform thickness (H=0.5 m), a series of extensive parametric study has been undertaken using the same FEM simulation procedures and mesh as shown in Table 2 and Figure 2, respectively. The parametric study was performed by changing only the deformation

modulus of the FRLTP ranging between 10 MPa and 250 MPa, while the improvement depth ratio of β=0.83 and the other properties of the FRLTP were remained unchanged. Figure 10 presents the variation of the SCR with an increase in the embankment height for various elastic deformation modulus of the FRLTP. As expected, an increase in the height of the embankment fill caused the initial increase in the SCR value subjected to the given embankment loading. This was followed by a gradual reduction of the SCR to a certain high value as the embankment height continuously increased to reach its final height of 6 m as illustrated in Figure 10. However, it is observed that the SCR value of the embankment reinforced with an FRLTP was certainly larger than that of the embankment without FRLTP. For example, during the embankment construction, when the height of the embankment fill increased from 0.5 m to 4 m, the SCR increased by approximately 50% as the deformation modulus of FRLTP increased from 10 MPa to 50 MPa. However, a further increase in the deformation modulus showed the negligible increase in the SCR for that given embankment height. Even though the decreasing trend of the SCR was observed in Figure 10 as the embankment height further increased to obtain its final height of 6 m, the SCR was higher for the FRLTP with higher deformation modulus. As Figure 10 shows, the effect of the FRLTP stiffness on the arching effect of the embankment was significant for the higher elastic deformation modulus of FRLTP (i.e. up to E=50 MPa), whereas the effect of the FRLTP Young's modulus greater than 50 MPa was negligible.

The effect of the FRLTP stiffness on the change of the differential settlement under the centre of the embankment is shown in Figure 11. It is found that for the FRLTP inclusion with a low deformation modulus of 10 MPa, the differential settlement at the completion at the embankment construction decreased by approximately 68% (from 125 mm to 40.5 mm) compared with that of the embankment without FRLTP. As the deformation modulus of the FRLTP increased to E=50 MPa, the corresponding differential settlement additionally reduced to 76%. However, a further increase in the FRLTP stiffness exceeded E=50 MPa led to a marginal improvement in the differential settlement. In other words, the effect of the FRLTP deformation modulus exceeded a certain value of E=50 MPa on the differential settlement was insignificant. Thus, an elastic deformation modulus of E=50 MPa is required to consider for the FRLTP design to support the given embankment height found on soft soils. Based on the numerical results presented in Figure 11, it can be concluded that the stiffness of the FRLTP showed a notable effect of the embankment differential settlement.

Figure 12 illustrates the change in the lateral displacement of a DCM column under the embankment toe along with depth at 2 years post-construction for the different FRLTP stiffness. The lateral displacement of the embankment without FRLTP is also illustrated in Figure 12 for reference.

It is observed that the lateral displacement of the embankment with FRLTP decreased gradually to a depth of around 2 m from the ground surface and then remained almost unchanged to a certain depth of 5 m. This was followed by a gradual increase again in the lateral deformation to the greater depth of 10 m (column tip) as shown in Figure 12. The larger lateral displacement was visually observed in Figure 12 for the embankment without FRLTP to the depth of around 5 m, and subsequently the difference in the lateral displacement between the embankment without and with FRLTP was negligible as the depth increased beyond 5 m. This phenomenon reconfirms that the effectiveness of the FRLTP inclusion in controlling the lateral deformation of the embankment at a shallow depth. A similar trend of the lateral displacement with depth was numerically predicted and reported by Zhang et al. (2013) for a geosynthetic reinforced and piles supported embankment. However, the numerical prediction results presented in Figure 12 indicate that the lateral displacement slightly increased with an increase in the elastic deformation modulus of the FRLTP from 10 MPa to 250 MPa although the increase in the lateral displacement appeared to be nominal. Referring to Figure 12, it is concluded that the stiffer FRLTP tended to show an adverse effect on the lateral resistance to the embankment deformation, but the adverse effect was insignificant.

4.3. Effect of the shear strength properties of FRLTP on the embankment behaviour

4.3.1. Effect of the FRLTP cohesion

To study the effect of the shear strength characteristics of FRLTP on the behaviour of the CS embankment with the same improvement depth ratio (β=0.83), a series of extensive parametric study was conducted by changing merely cohesion value of the FRLTP ranging between 10 kPa and 300 kPa, while the other properties of the FRLTP were remained unchanged. The predicted results of the parametric study were plotted in Figure 13-15 showing the variations of the SCR, the differential settlement of the ground surface against the embankment height, and the lateral displacement with depth, respectively. Figure 13 reveals that the SCR increased with an increase in cohesion of the FRLTP and embankment height to a great extent. It is observed that increasing the FRLTP cohesion value from 10 kPa to 75 kPa led to a remarkable increase in the SCR value from roughly 5 to between 20 and 98 when the embankment height increased from 0.5 m to 4 m. This behaviour was followed by a decrease in the SCR value to a certainly high value (e.g. an SCR of 50 for the FRLTP cohesion of 75 kPa) with the increase in embankment height greater than 4 m, as depicted in Figure 13. A drop in the SCR value showed an indication of the increase in differential settlement of the ground surface due to the over-bearing capacity of the DCM columns induced by increasing the embankment height.

However, the further increase in the FRLTP cohesion value up to 150 kPa and 300 kPa, respectively, exhibited a linearly significant increase in the SCR to a great value of around 150 without presenting a decreased in the SCR value as the embankment height increased from 0.5 m to its final height of 6 m. The higher SCR value is most likely to promote the better embankment load transfer from foundation soil to DCM columns due to the enhancement of arching effect and consequently prevent the development of the differential settlement of the ground surface as the following discussion. However, the FRLTP cohesion value of 300 kPa did not produce the greater SCR value compared with the 150 kPa cohesion of the FRLTP irrespective of any of the embankment height. This implies that the lime-fibre-soil having a high cohesion of 150 kPa reached an optimum value to be adopted as an FRLTP, further increase in the FRLTP cohesion would not generate a significant effect on the SCR of the embankment.

In addition, the effect of the FRLTP cohesion of the differential settlement of the ground surface can be seen in Figure 14. Similar to the trend of SCR, an increase in cohesion of the FRLTP resulted in the improvement in the differential settlement of the ground surface caused by the increase in the embankment height. For example, the increase in cohesion from 10 kPa to 150 kPa resulted in the significant reduction in the maximum differential settlement ranging from roughly 80 mm to 6 mm, which yielded approximately 92% reduction of the differential settlement. However, the higher increase in the FRLPT cohesion up to 300 kPa produced the insignificant decrease in the maximum differential settlement to a certainly low level of around 4 mm as the embankment height increased up to 6 m. Thus, it can be concluded that the FRLTP cohesion is highly effective in controlling the differential ground surface settlement. The FRLTP cohesion of 150 kPa or greater could minimise almost the entire differential settlement induced by the certain embankment height.

Figure 15 shows the effect on the FRLTP cohesion on the lateral displacement with depth of the DCM column under the embankment toe at 2 years post-construction. As illustrated in Figure 15, the lateral displacement of the embankment with FRLTP significantly reduced to a small value (around 5 mm at the column head) when the FRLTP cohesion increased from 10 kPa to 300 kPa, which means the higher cohesion of the FRLTP can control zero lateral deformation of the embankment toe. Moreover, the increase of the FRLTP cohesion reveals a notable influence on the lateral displacement of the CS embankment to a certain depth of around 5 m from the ground surface and then it exhibits an insignificant impact on the lateral deformation to a greater depth. As Figure 15 shows, the embankment without FRLTP obviously illustrated the larger lateral displacement in comparison with the embankment with FRLTP. This numerical prediction indicates that the FRLTP cohesion has a significant effect on the lateral resistance to the embankment deformation.

4.3.2. Effect of the FRLTP friction angle

Another series of the parametric study was undertaken by only varying the internal friction angle of the FRLTP ranging between 1° and 42° together with an increase in the embankment height. Meanwhile, the cohesion value of 75 kPa, the improvement depth ratio (β=0.83), and other properties of the FRLTP were kept constant as shown in Figure 1. The fluctuations of the SCR, the differential settlement and the lateral deformation against the embankment height for different friction angles of the FRLTP were presented in Figure 16-18, respectively. In overall, the SCR value as shown in Figure 16 increased to a great value as the embankment height increased. This was followed by a drop in the SCR value to a certainly high level, which can clearly be observed in any cases of the FRLTP friction angle. Dissimilar to the trend of SCR caused by the increase in the FRLTP cohesion, the increase in the FRLTP fiction angle produced almost the same SCR values as the embankment height increased from 0.5 m to 3 m. Following, when the embankment height increased higher than 3 m, the SCR tended to decrease after approaching a peak around 4 m of the embankment height. Although the SCR decrease was observed for the embankment height exceeded 4 m, a greater SCR value was clearly observed for the higher friction angle of the FRLTP. However, Figure 16 reveals that the increase in the FRLTP friction angle higher than 30° resulted in an insignificant improvement in the SCR value.

Furthermore, the effect of the FRLTP friction angle on the differential settlement of the ground surface can be observed in Figure 17. Generally, observation of the predicted results in Figure 17 indicates that an increase in the embankment from 0.5 m to 3 m caused a minimal increase in the differential settlement of the ground surface. Moreover, the increase in the FRLTP friction angle from 1° to 42° showed no notable effect on the improvement in the differential settlement in that range of the embankment height. Nonetheless, when the embankment height increased further from 3 m to 6 m, an increase in the FRLTP friction angle from 1° to 30° led to a decrease in the differential settlement of the ground surface from 60 mm to approximately 30 mm. The additional increase in the FRLTP friction angle exceeded 30° revealed the insignificant improvement or even resulted in the slight increase in the differential settlement as presented in Figure 17. It can be concluded that the increase in friction angle of the FRLTP effectively promoted the improvement in the SCR and the differential settlement on the ground surface. However, when comparing with the FRLTP cohesion, the improvement in the SCR and the differential settlement of the investigated embankment is more

dominant for the increase in the FRLTP cohesion than those subjected to the increase in the FRLTP friction angle.

The influence on the FRLTP friction angle on the 2 years post-construction lateral displacement with depth of the DCM column under the embankment toe is shown in Figure 18. It can be seen that when the FRLTP friction angle increased from 1° to 42°, the lateral displacement of the embankment with FRLTP decreased considerably and nonlinearly with depth. For example, the corresponding reduction of the lateral displacement of column head was from approximately 100 mm for the FRLTP friction angle of 1° to about 60 mm for the FRLTP friction angle of 42°, resulting in the significant improvement in the lateral deformation at the embankment toe by around 40%. However, the additional increase in the FRLTP friction angle beyond 42° yielded a negligible improvement in the embankment lateral displacement. Similar to the trend of the lateral displacement of the CS embankment associated with the fluctuations of FRLTP cohesion, the influence of the FRLTP friction angle changes on the lateral deformation was found to take place to a shallow depth of around 5 m from the ground surface. Afterwards, its influence on the lateral deformation was negligible as the depth increased further to the DCM columns tip. It is also noted that the predicted lateral displacement of the embankment without FRLTP was visibly larger compared to the embankment reinforced with an FRLTP. Referring to Figure 18, it can be concluded that the effect of the FRLTP friction angle on the 2 years post-construction lateral displacement of the CS embankment was significant.

4.4. Effect of the tensile strength properties of FRLTP on the embankment behaviour

The effect of the tensile strength characteristics of FRLTP on the embankment behaviour with the same improvement depth ratio (β=0.83) was numerically investigated by varying the only tensile strength value of the FRLTP ranging between 10 kPa and 240 kPa, while the other properties of the FRLTP were kept constant. As observed in Figure 19, the SCR increased with the embankment height but decreased with increasing the FRLTP tensile strength. The SCR difference associated with the increase in the FRLTP tensile strength from 10 kPa and 240 kPa can visibly be observed when the embankment height increased from 4 m to 6 m during the construction process. As Figure 19 illustrates, the reduction of the SCR indicated the decrease in the arching effect of the embankment as the FRLTP tensile strength increased. Consequently, this resulted in the corresponding increase in the embankment (differential) settlement as shown in Figure 20 since the more embankment load transferred to foundation soils. Although the embankment SCR was greater and the differential

settlement was smaller for the embankment with the higher FRLTP tensile strength when comparing the embankment without FRLTP as presented in Figure 19 and 20, the predicted results of this parametric study revealed that the influence of the FRLRP tensile strength increase became negative.

Figure 21 shows that the increase in the FRLTP tensile strength becomes very effective in improving the lateral displacement of the embankment with depth. As illustrated in Figure 21, the post-construction lateral deformation of the embankment toe decreased by approximately 52% as the FRLTP tensile strength increased from 10 kPa to 125 kPa. Meanwhile, a further increase in the FRLTP tensile strength up to 240 kPa yielded an insignificant effect on the improvement in the lateral deformation. Therefore, a tensile strength of 125 kPa is required to consider for the FRLTP design in support of the 6 m embankment height built columns improved soft soils. The improvement of the lateral displacement could be attributed to the higher tensile strength of FRLTP that facilities the better resistance to the lateral spreading forces caused by an increase in the height of the embankment fill and consequently reduces the lateral earth pressure acting on the DCM columns with depth.

4.5. Limitations and future work

The thickness of the FRLTP plays an essential role in facilitating the embankment load to be effectively transferred to the DCM columns from soft foundation soil, enhancing the rigidity and stability of the embankment system, and reducing the possibility of the FRLTP punching failure induced by column heads. Through a previous numerical analysis accomplished by the authors (Dang et al. 2018b), the results revealed that the embankment with various FRLTP thickness of 0.5-3 m as compared with the embankment without FRLTP could effectively reduce the total and differential settlements, and the lateral displacement of the embankment by 32%, 100% and 83%, respectively. Therefore, investigating the effects of different FRLTP thicknesses on behaviour of the floating DCM columns supported embankment were beyond the scope of this study. Moreover, this current investigation draws its primary attention to the mechanical properties of the FRLTP to support embankment, a novel ground modification technique, but does not take into consideration of the effects of the other design parameters of a typical columns-embankment system on soft soils such as shear strength, stiffness, and permeability of soft soils below embankment as well as the columns stiffness, the columns diameter, and the columns distance ratio. This is because the effects of such other design parameters on the behaviour of a CS embankment reinforced without or with a platform (e.g. geosynthetics) could be found in previous publications (Chai et al. 2015; Chai et al. 2017; Han & Gabr 2002; Yapage & Liyanapathirana 2014), well-documented in the literature. However, further investigations are required to assess the efficiency and the interaction between DCM columns,

FRLTP and soft foundation soils by taking into account the design parameters mentioned above to fully understand the performance of a CS embankment reinforced with FRLTP during embankment construction and serviceability. Finally, a relationship between the improvement depth ratio (β) and other design parameters could be important, but it was identified as a follow-up study and beyond the scope of this paper because of the extensiveness of the current work.

5. CONCLUSIONS

This paper has presented a numerical investigation on the behaviour of fibre reinforced load transfer platform (FRLTP) and deep cement mixing (DCM) columns supported embankments constructed on multilayers of soft soils. An equivalent 2D plane strain finite element method was adopted to evaluate the behaviour of the embankment without or with FRLTP. An extensive parametric study on the full geometry of the DCM columns supported embankment was also numerically carried out to further investigate the influence of the FRLTP parameters such as the elastic deformation modulus (Young's modulus), the shear strength properties and the tensile strength, and the soft soil improvement depth on the performance of the embankment during construction and post-construction periods. The main findings of this numerical study can be summarised as follows:

- Comparing with the DCM columns supported embankment without FRLTP, the numerical results indicated that the application of the FRLTP combined with DCM columns supported embankment can minimise the total settlement significantly, meanwhile effectively alleviate the lateral displacement and consequently increase the stability of the entire embankment system built over multilayers of soft soils. Furthermore, the embankment with FRLTP can not only enhance the stress concentration ratio (SCR) between DCM columns and surrounding soils to a great extent but also accelerate the consolidation progress subjected to embankment load.
- The findings of the parametric study confirm that the improvement depth ratio has significant effects on the total and differential settlements, the load transfer mechanism between DCM columns and foundation soils via the enhancement of the SCR, and the lateral displacement of the embankment during the construction and post-construction time. Moreover, the elastic deformation modulus of the FRLTP had considerable effects on the differential settlement, the SCR but showed a negligible effect on the lateral deformation of the investigated embankment.
- The numerical results derived from the parametric study on the FRLTP shear strength properties also indicates that the cohesion and the internal friction angle of the FRLTP have significant effects on improving the SCR, the lateral displacement, and the differential settlement of the

investigated embankment. However, the improvement in the overall performance of the embankment dependent on the shear strength properties was more pronounced for the cohesion of the FRLTP.

- The predicted results of this numerical modelling reveal that the tensile strength of the FRLTP has considerable effects on the lateral displacement of the investigated embankment, but shows negative impacts on the SCR and the differential settlement.
- This numerical modelling also confirms that the application of eco-friendly and recycled fibre-lime reinforced soil can effectively be used as an alternative green load transfer platform combined with DCM columns supported embankments built on top of multilayered soft soils due to the significant improvement in the SCR, the total and differential settlements, and the lateral displacement of the examined embankment. It should be noted that this finding was primarily derived from the comparison between the columns supported embankments without and with FRLTP. Meanwhile, the assessment of the potential replacement of geosynthetics by FRLTP supported embankments was not elaborated in this paper, as it can be found in the previous publication by the authors (Dang et al. 2016a).
- Finally but most importantly, this numerical investigation has explored an interesting potential for making use of agricultural waste by-products such as coconut coir fibre, jute fibre and bagasse fibre as construction fill materials for sustainable civil infrastructure development.

6. ACKNOWLEDGEMENTS

The results presented in this paper are part of an ongoing research at University of Technology Sydney (UTS), partially funded by the Australian Technology Network and Arup Pty Ltd. The authors gratefully acknowledge their support.

7. REFERENCES

Anggraini, V., Asadi, A., Huat, B.B.K. & Nahazanan, H. 2015, 'Performance of Chemically Treated Natural Fibres and Lime in Soft Soil for the Utilisation as Pile-Supported Earth Platform', *International Journal of Geosynthetics and Ground Engineering*, vol. 1, no. 3, pp. 1-14.

Ariyarathne, P., Liyanapathirana, D. & Leo, C. 2013, 'Comparison of Different Two-Dimensional Idealizations for a Geosynthetic-Reinforced Pile-Supported Embankment', *International Journal of Geomechanics*, vol. 13, no. 6, pp. 754-68.

CDIT 2002, *The Deep Mixing Method: Principle, Design and Construction*, CRC Press/Balkema The Netherlands.

Chai, J.-C., Shrestha, S., Hino, T., Ding, W.-Q., Kamo, Y. & Carter, J. 2015, '2D and 3D analyses of an embankment on clay improved by soil–cement columns', *Computers and Geotechnics*, vol. 68, pp. 28-37.

Chai, J.-c., Shrestha, S., Hino, T. & Uchikoshi, T. 2017, 'Predicting bending failure of CDM columns under embankment loading', *Computers and Geotechnics*, vol. 91, pp. 169-78.
Chen, Q. & Indraratna, B. 2014, 'Shear behaviour of sandy silt treated with lignosulfonate', *Canadian Geotechnical Journal*, vol. 52, no. 8, pp. 1180-5.
Consoli, N.C., Casagrande, M.D.T., Thomé, A., Rosa, F.D. & Fahey, M. 2009a, 'Effect of relative density on plate loading tests on fibre-reinforced sand', *Géotechnique*, vol. 59, no. 5, pp. 471-6.
Consoli, N.C., Vendruscolo, M.A., Fonini, A. & Rosa, F.D. 2009b, 'Fiber reinforcement effects on sand considering a wide cementation range', *Geotextiles and Geomembranes*, vol. 27, no. 3, pp. 196-203.
Dang, L.C. 2018, 'Enhancing the Engineering Properties of Expansive Soil Using Bagasse Ash, Bagasse Fibre and Hydrated Lime', Ph.D. thesis, University of Technology Sydney.
Dang, L.C., Dang, C., Fatahi, B. & Khabbaz, H. 2016a, 'Numerical Assessment of Fibre Inclusion in a Load Transfer Platform for Pile-Supported Embankments over Soft Soil', *Geo-China 2016*, eds D. Chen, J. Lee & W.J. Steyn, vol. GSP 266, ASCE, pp. 148-55.
Dang, L.C., Dang, C.C. & Khabbaz, H. 2017a, 'Behaviour of Columns and Fibre Reinforced Load Transfer Platform Supported Embankments Built on Soft Soil', *the 15th International Conference of the International Association for Computer Methods and Advances in Geomechanics*, Wuhan, China.
Dang, L.C., Dang, C.C. & Khabbaz, H. 2018a, 'Numerical Analysis on the Performance of Fibre Reinforced Load Transfer Platform and Deep Mixing Columns Supported Embankments', in M. Bouassida & M.A. Meguid (eds), *Ground Improvement and Earth Structures*, Springer, Cham, pp. 157-69.
Dang, L.C., Dang, C.C. & Khabbaz, H. 2018b, 'A Parametric Study of Deep Mixing Columns and Fibre Reinforced Load Transfer Platform Supported Embankments', in H. Khabbaz, H. Youn & M. Bouassida (eds), *New Prospects in Geotechnical Engineering Aspects of Civil Infrastructures*, Springer, Cham, pp. 179-94.
Dang, L.C., Fatahi, B. & Khabbaz, H. 2016b, 'Behaviour of Expansive Soils Stabilized with Hydrated Lime and Bagasse Fibres', *Procedia Engineering*, vol. 143, pp. 658-65.
Dang, L.C., Hasan, H., Fatahi, B., Jones, R. & Khabbaz, H. 2016c, 'Enhancing the Engineering Properties of Expansive Soil Using Bagasse Ash and Hydrated Lime', *International Journal of GEOMATE*, vol. 11, no. 25, pp. 2447-54.
Dang, L.C., Hasan, H., Fatahi, B. & Khabbaz, H. 2015, 'Influence of Bagasse Ash and Hydrated Lime on Strength and Mechanical Behaviour of Stabilised Expansive Soil', *GEOQuébec 2015*, Québec City, Canada.
Dang, L.C. & Khabbaz, H. 2018a, 'Assessment of the geotechnical and microstructural characteristics of lime stabilised expansive soil with bagasse ash', *GeoEdmonton 2018*, Alberta, Canada.
Dang, L.C. & Khabbaz, H. 2018b, 'Enhancing the Strength Characteristics of Expansive Soil Using Bagasse Fibre', *Springer Series in Geomechanics and Geoengineering*, Springer, Cham, pp. 792-6.
Dang, L.C. & Khabbaz, H. 2018c, 'Shear strength behaviour of bagasse fibre reinforced expansive soil', *IACGE2018*, vol. Geotechnical Special Publications, ASCE, Chongqing, China.
Dang, L.C. & Khabbaz, H. 2019, 'Experimental Investigation on the Compaction and Compressible Properties of Expansive Soil Reinforced with Bagasse Fibre and Lime', in J.S. McCartney & L.R. Hoyos (eds), *Recent Advancements on Expansive Soils*, Springer, Cham, pp. 64-78.
Dang, L.C., Khabbaz, H. & Fatahi, B. 2017b, 'Evaluation of swelling behaviour and soil water characteristic curve of bagasse fibre and lime stabilised expansive soil', *PanAm-UNSAT 2017*, vol. GSP 303, ASCE, Texas, USA, pp. 58-70.
Dang, L.C., Khabbaz, H. & Fatahi, B. 2017c, 'An experimental study on engineering behaviour of lime and bagasse fibre reinforced expansive soils', *19th ICSMGE*, Seoul, Republic of Korea, pp. 2497-500.
Dang, L.C., Khabbaz, H. & Hasan, H. 2018c, 'Geotechnical Characteristics of Expansive Soils Stabilised with Bagasse Ash and Hydrated Lime', *Soils and Foundations (under review)*.
Fatahi, B., Basack, S., Premananda, S. & Khabbaz, H. 2012, 'Settlement prediction and back analysis of Young's modulus and dilation angle of stone columns', *Australian Journal of Civil Engineering*, vol. 10, no. 1, p. 67.
Fatahi, B. & Khabbaz, H. 2013, 'Influence of fly ash and quicklime addition on behaviour of municipal solid wastes', *Journal of Soils and Sediments*, vol. 13, no. 7, pp. 1201-12.

Fatahi, B. & Khabbaz, H. 2015, 'Influence of Chemical Stabilisation on Permeability of Municipal Solid Wastes', *Geotechnical and Geological Engineering*, vol. 33, no. 3, pp. 455–66.
Filz, G.M. & Navin, M.P. 2006, *Stability of column-supported embankments*, Virginia Transportation Research Council, Charlottesville, VA., Report No. VTRC 06-CR13.
Han, J. & Gabr, M. 2002, 'Numerical Analysis of Geosynthetic-Reinforced and Pile-Supported Earth Platforms over Soft Soil', *Journal of Geotechnical and Geoenvironmental Engineering*, vol. 128, no. 1, pp. 44-53.
Huang, J. & Han, J. 2010, 'Two-dimensional parametric study of geosynthetic-reinforced column-supported embankments by coupled hydraulic and mechanical modeling', *Computers and Geotechnics*, vol. 37, no. 5, pp. 638-48.
Jamsawang, P., Yoobanpot, N., Thanasisathit, N., Voottipruex, P. & Jongpradist, P. 2016, 'Three-dimensional numerical analysis of a DCM column-supported highway embankment', *Computers and Geotechnics*, vol. 72, pp. 42-56.
Liu, H., Ng, C. & Fei, K. 2007, 'Performance of a Geogrid-Reinforced and Pile-Supported Highway Embankment over Soft Clay: Case Study', *Journal of Geotechnical and Geoenvironmental Engineering*, vol. 133, no. 12, pp. 1483-93.
Liu, K.W. & Rowe, R.K. 2015, 'Numerical modelling of prefabricated vertical drains and surcharge on reinforced floating column-supported embankment behaviour', *Geotextiles and Geomembranes*, vol. 43, no. 6, pp. 493-505.
Martin, J., Collins, R., Browning, J. & Biehl, F. 1990, 'Properties and Use of Fly Ashes for Embankments', *Journal of Energy Engineering*, vol. 116, no. 2, pp. 71-86.
Nguyen, B.T.T., Takeyama, T. & Kitazume, M. 2016, 'Numerical analyses on the failure of deep mixing columns reinforced by a shallow mixing layer', *Japanese Geotechnical Society Special Publication*, vol. 2, no. 63, pp. 2144-8.
Okyay, U.S. & Dias, D. 2010, 'Use of lime and cement treated soils as pile supported load transfer platform', *Engineering Geology*, vol. 114, no. 1–2, pp. 34-44.
Parsa-Pajouh, A., Fatahi, B. & Khabbaz, H. 2015, 'Experimental and Numerical Investigations to Evaluate Two-Dimensional Modeling of Vertical Drain–Assisted Preloading', *International Journal of Geomechanics*, vol. 16, no. 1, p. B4015003.
Tan, S., Tjahyono, S. & Oo, K. 2008, 'Simplified Plane-Strain Modeling of Stone-Column Reinforced Ground', *Journal of Geotechnical and Geoenvironmental Engineering*, vol. 134, no. 2, pp. 185-94.
Tang, C., Shi, B., Gao, W., Chen, F. & Cai, Y. 2007, 'Strength and mechanical behavior of short polypropylene fiber reinforced and cement stabilized clayey soil', *Geotextiles and Geomembranes*, vol. 25, no. 3, pp. 194-202.
Terzaghi, K. 1943, *Theoretical soil mechanics*, vol. 18, Wiley New York.
Venda Oliveira, P.J., Pinheiro, J.L.P. & Correia, A.A.S. 2011, 'Numerical analysis of an embankment built on soft soil reinforced with deep mixing columns: Parametric study', *Computers and Geotechnics*, vol. 38, no. 4, pp. 566-76.
Wang, Y.-X., Guo, P.-P., Ren, W.-X., Yuan, B.-X., Yuan, H.-P., Zhao, Y.-L., Shan, S.-B. & Cao, P. 2017, 'Laboratory Investigation on Strength Characteristics of Expansive Soil Treated with Jute Fiber Reinforcement', *International Journal of Geomechanics*, vol. 17, no. 11, p. 04017101.
Yapage, N., Liyanapathirana, D., Kelly, R., Poulos, H. & Leo, C. 2014, 'Numerical Modeling of an Embankment over Soft Ground Improved with Deep Cement Mixed Columns: Case History', *Journal of Geotechnical and Geoenvironmental Engineering*, vol. 140, no. 11, p. 04014062.
Yapage, N., Liyanapathirana, D., Poulos, H., Kelly, R. & Leo, C. 2015, 'Numerical Modeling of Geotextile-Reinforced Embankments over Deep Cement Mixed Columns Incorporating Strain-Softening Behavior of Columns', *International Journal of Geomechanics*, vol. 15, no. 2, p. 04014047.
Yapage, N.N.S. & Liyanapathirana, D.S. 2014, 'A parametric study of geosynthetic-reinforced column-supported embankments', *Geosynthetics International*, vol. 21, no. 3, pp. 213-32.
Zhang, J., Zheng, J.-J., Chen, B.-G. & Yin, J.-H. 2013, 'Coupled mechanical and hydraulic modeling of a geosynthetic-reinforced and pile-supported embankment', *Computers and Geotechnics*, vol. 52, pp. 28-37.

LIST OF TABLES

Table 1. Material properties of the embankment, FRLTP, DCM columns and subgrade soil layers

Parameters	Surface layer	Soft clay 1	Soft clay 2	Stiff clay	Sandy clay	Fibre-lime-soil	Embankment fill	DCM columns
Depth (m)	0-1	1-4	4-12	12-15	15-30	-	-	-
Material model	MCC*	MCC	MCC	MCC	MC*	MC	MC	MC
Unit weight γ (kN/m^3)	16	13.4	14.3	18	19	12.5	19	15
Young's modulus, E (MPa)	-	-	-	-	20	125.8	1	100
Poisson's ratio, ν	0.15	0.15	0.15	0.15	0.10	0.32	0.40	0.15
Effective cohesion, c' (kPa)	-	-	-	-	20	75	20	c_u=500
Effective friction angle, φ' (°)	-	-	-	-	35	42	35	0
Compression index,λ	0.25	0.87	0.43	0.12	-	-	-	-
Swelling index, κ	0.025	0.087	0.043	0.012	-	-	-	-
Over consolidation ratio, OCR	1.5	2.5	1.2	1.0	-	-	-	-
Slope of the critical state line, M	1.2	1.2	1.2	1.4	-	-	-	-
Initial void ratio, e_0	1.5	3.1	2.49	0.8	0.7	-	-	-
Vertical Permeability coefficient, k_v (m/day)	6×10^{-4}	4.4×10^{-4}	4.6×10^{-4}	2.5×10^{-3}	2.5×10^{-2}	-	-	4.6×10^{-4}
Horizontal Permeability coefficient, k_h (m/day)	9.1×10^{-4}	6.6×10^{-4}	6.9×10^{-4}	2.5×10^{-3}	2.5×10^{-2}	-	-	4.6×10^{-4}
Material behaviour	Undrained	Undrained	Undrained	Undrained	Drained	Undrained	Drained	Undrained type B

*MC: Mohr-Coulomb; MCC: Modified Cam Clay

Table 2. Construction stages in the FEM simulation of embankment construction procedure

Stage	Description	Thickness (m)	Duration (days)
1	Generation on the initial stresses (Ko- condition)	-	-
2	Installation of the DCM columns	-	-
3	Construction of a 0.5 m high embankment	0.5	8
4	Construction of a 1.0 m high embankment	0.5	8
5	Construction of a 2.0 m high embankment	1.0	16
6	Construction of a 3.0 m high embankment	1.0	16
7	Construction of a 4.0 m high embankment	1.0	16
8	Construction of a 5.0 m high embankment	1.0	16
9	Construction of a 6.0 m high embankment	1.0	20
10	Consolidation period of 2 years	-	730

LIST OF FIGURES

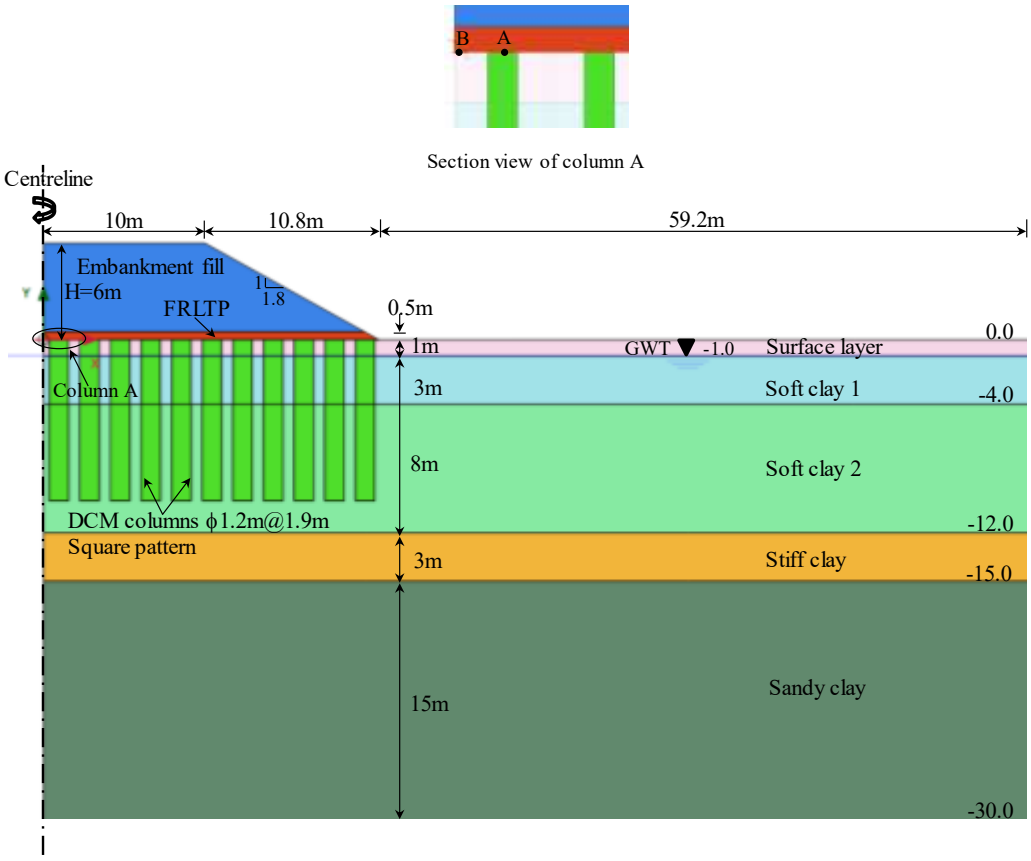

Figure 1 Cross section of the fibre reinforced load transfer platform and DCM columns supported embankment

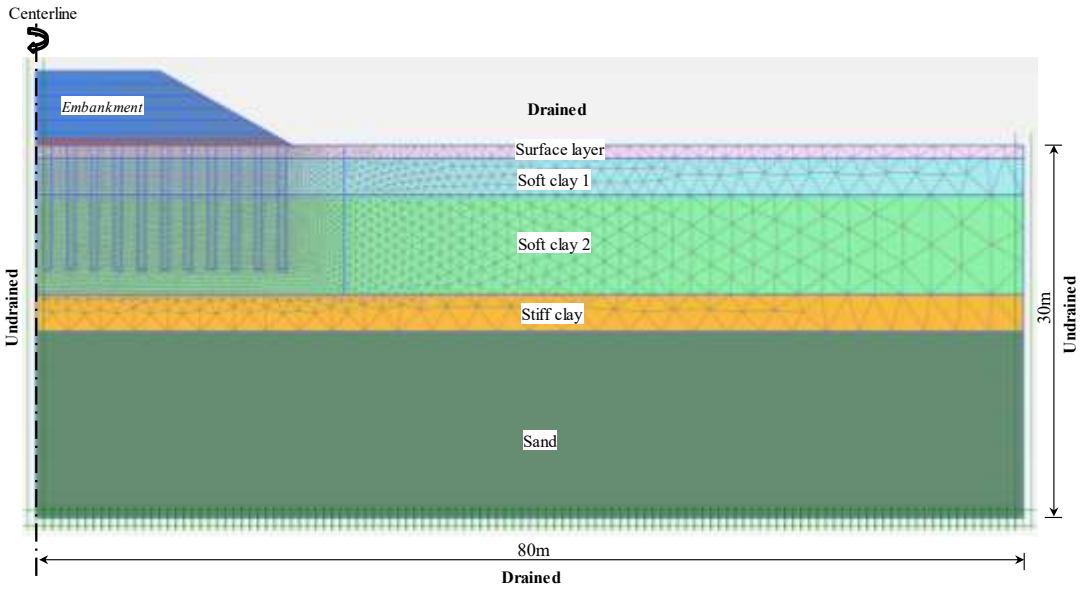

Figure 2 Mesh and boundary conditions for an equivalent 2D FEM analysis of embankment

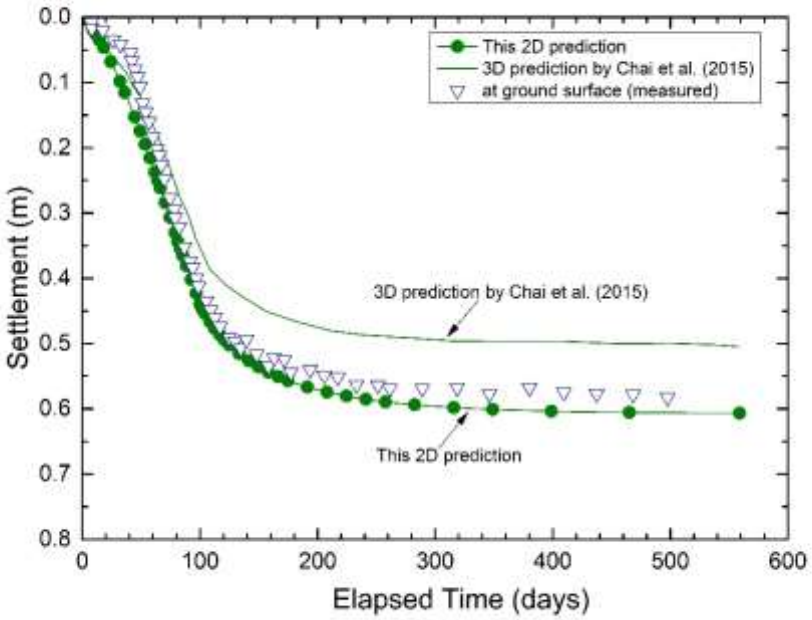

(a)

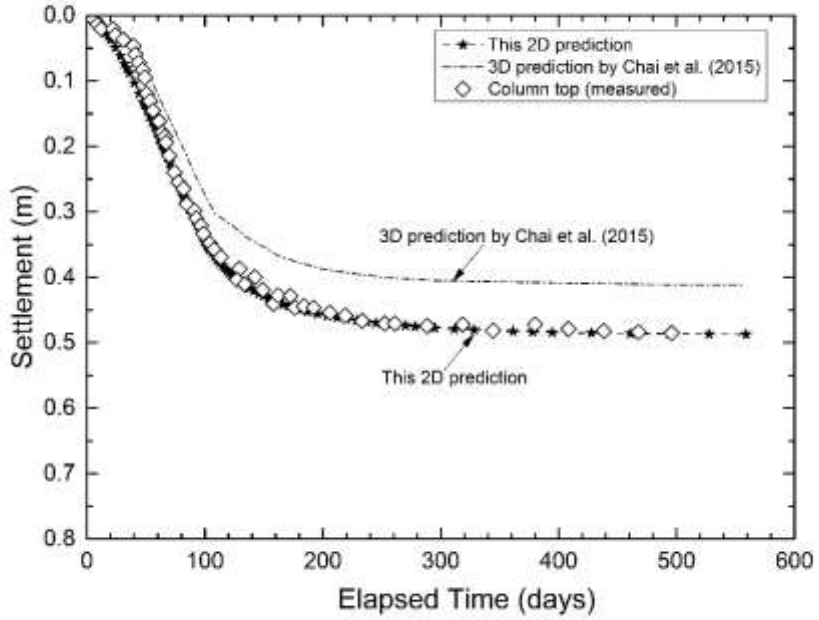

(b)

Figure 3 Comparison between field measurements, 2D and 3D numerical predictions of the embankment settlement at (a) ground surface and (b) column top with time

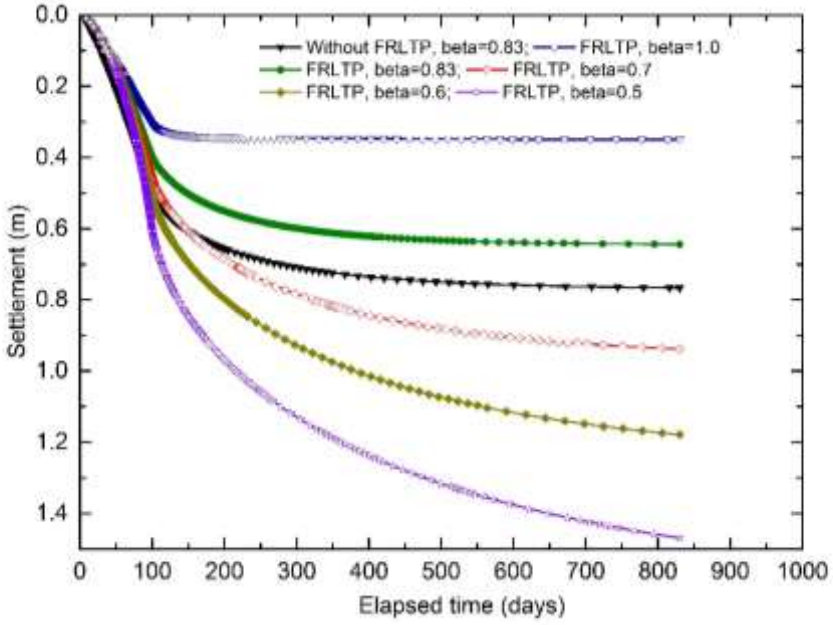

(a)

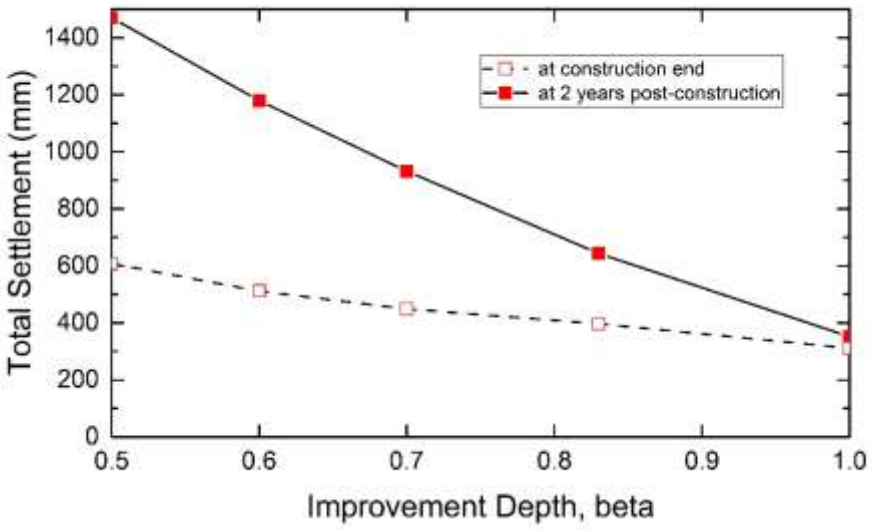

(b)

Figure 4 Development of (a) total settlement with time and (b) total settlement at embankment construction completion and 2 years post-construction for different improvement depth ratios (β)

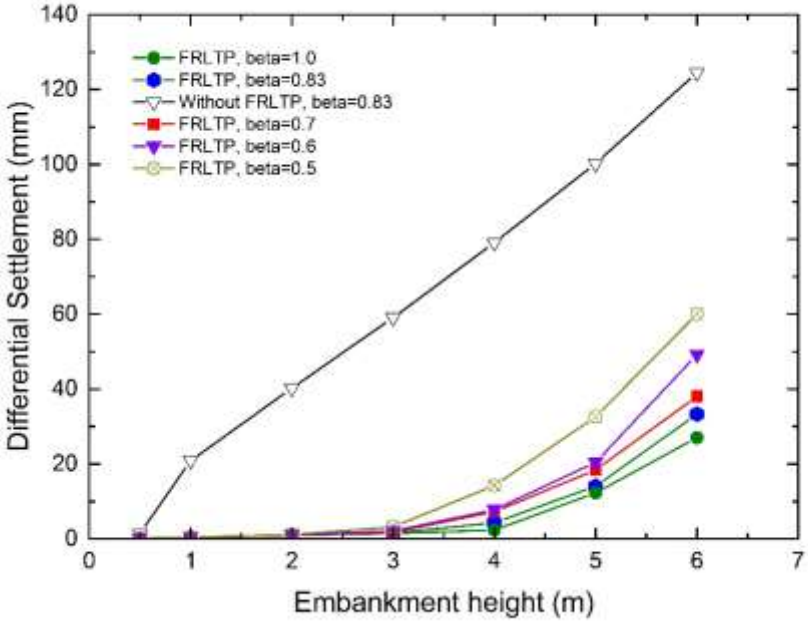

Figure 5 Variation of differential settlement versus embankment height for different improvement depth ratios (β)

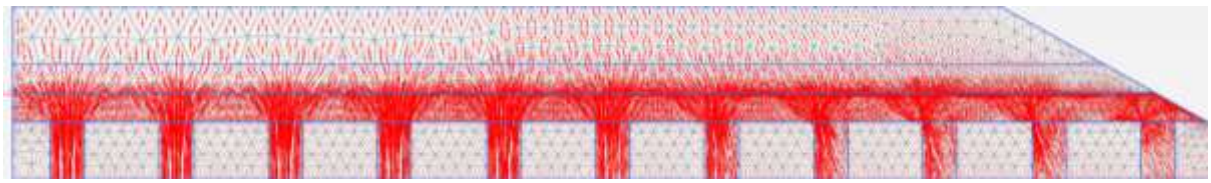

(a)

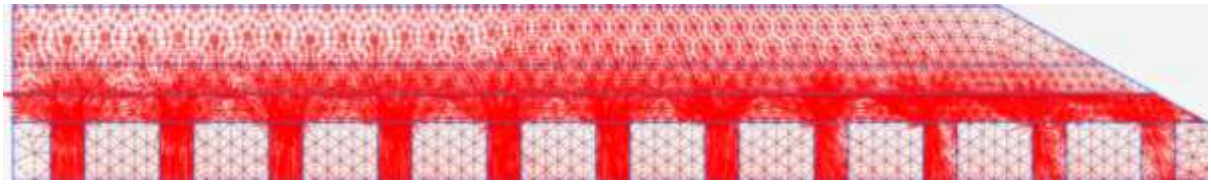

(b)

Figure 6 Effective principle stresses of the embankment with FRLTP at the construction end for the improvement depth ratios of (a) β=0.5 and (b) β=0.83

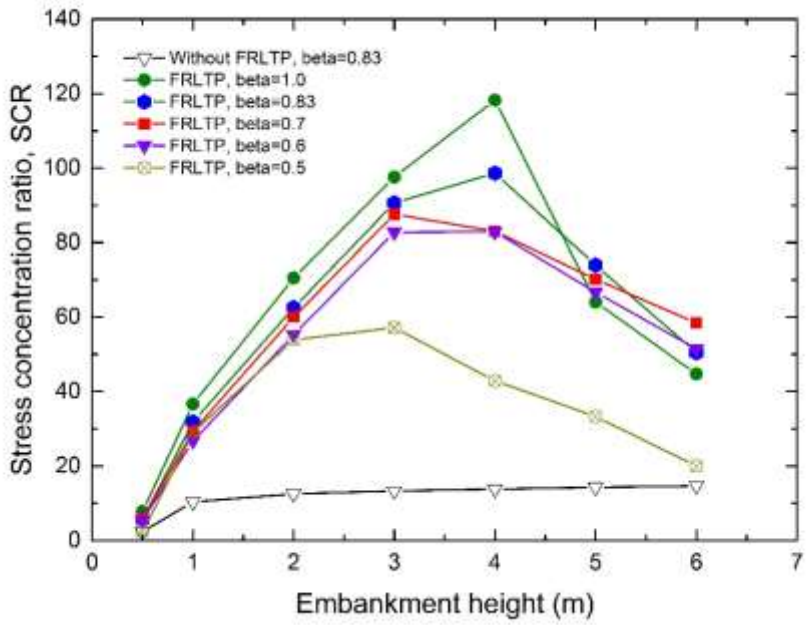

Figure 7 Variation of stress concentration ratio with embankment height for different improvement depth ratios (β)

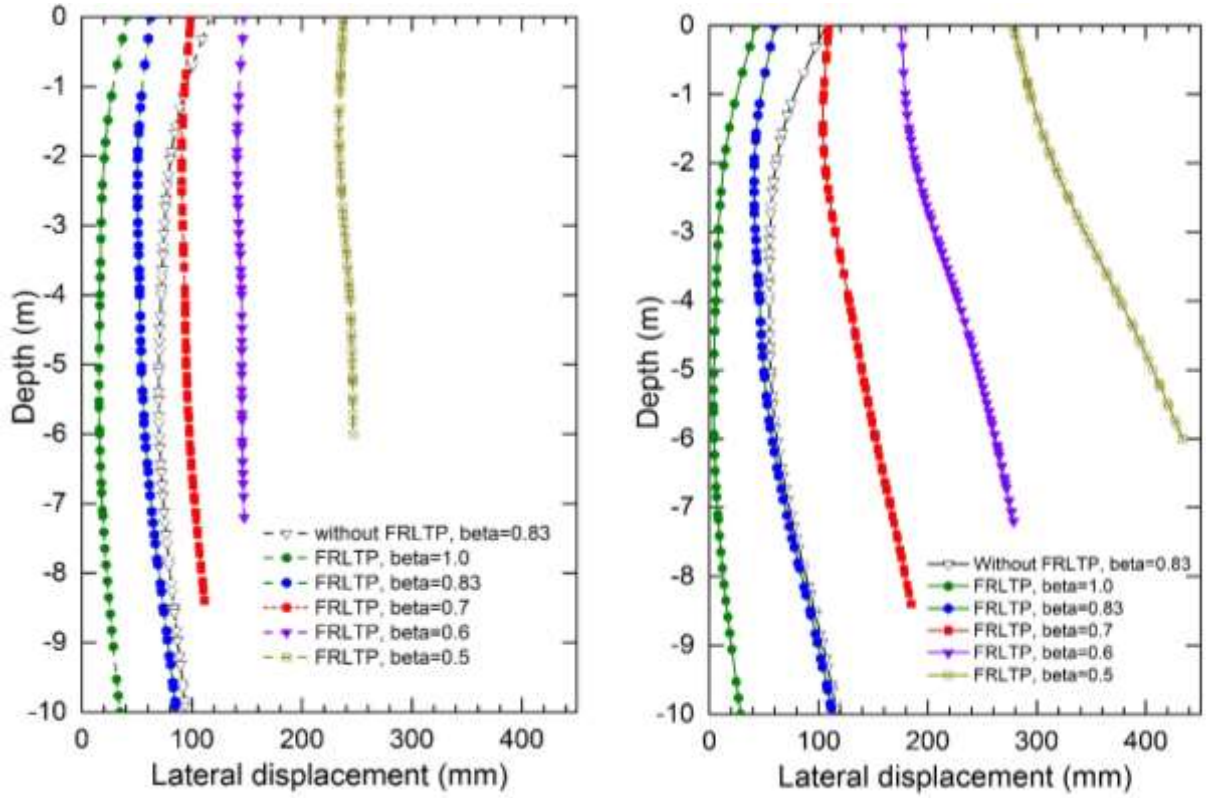

(a) (b)

Figure 8 Variation of lateral displacement with depth for different improvement depth ratios (β) at (a) completion of embankment construction and (b) 2 years post-construction

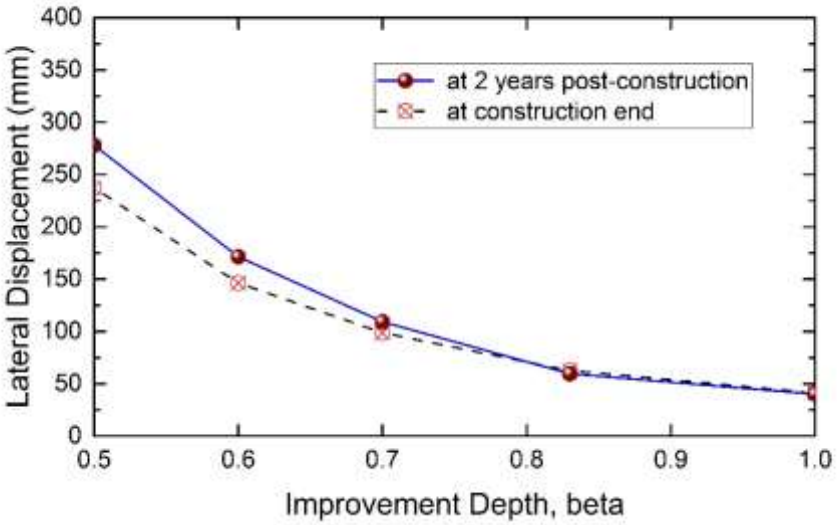

Figure 9 Variation of lateral displacement of the embankment toe for different improvement depth ratio at embankment construction completion and 2 years post-construction

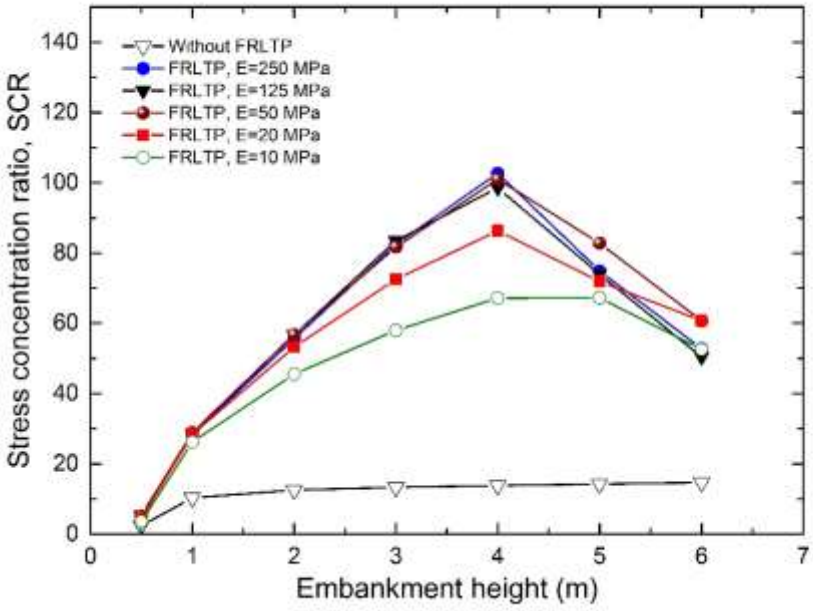

Figure 10 Effect of FRLTP Young's modulus variation on stress concentration ratio (SCR)

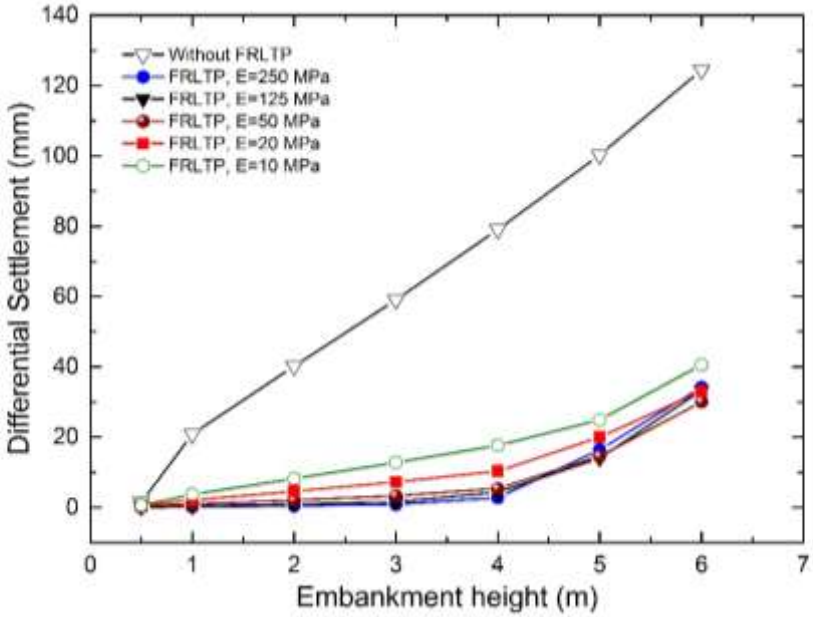

Figure 11 Effect of elastic deformation modulus of FRLTP on differential settlement

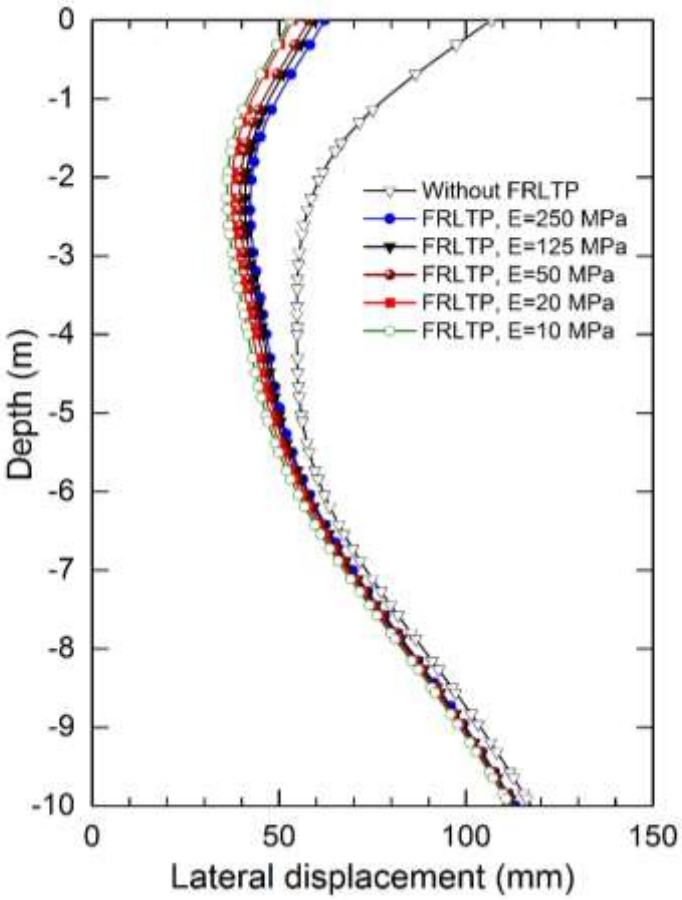

Figure 12 Variation of the lateral displacement with depth for various elastic deformation modulus of FRLTP at 2 years post-construction

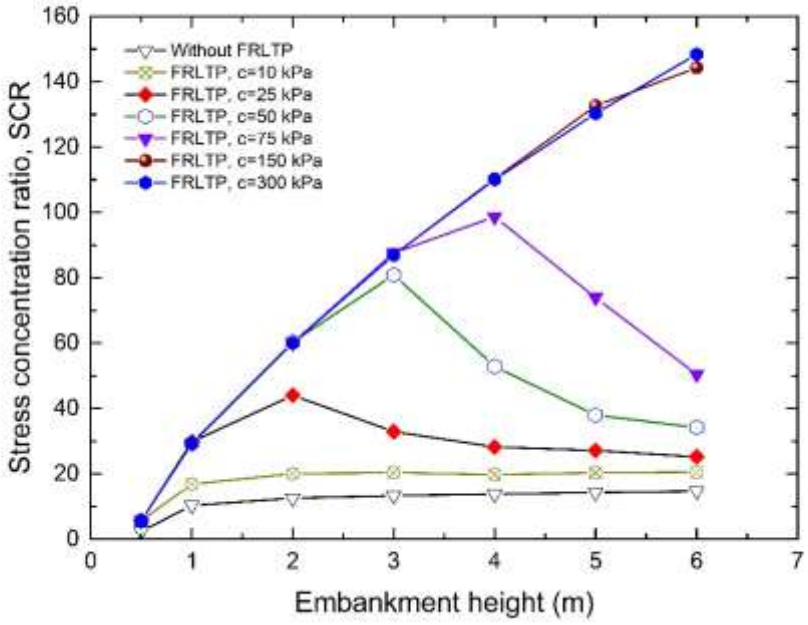

Figure 13 Effect of the FRLTP cohesion on stress concentration ratio

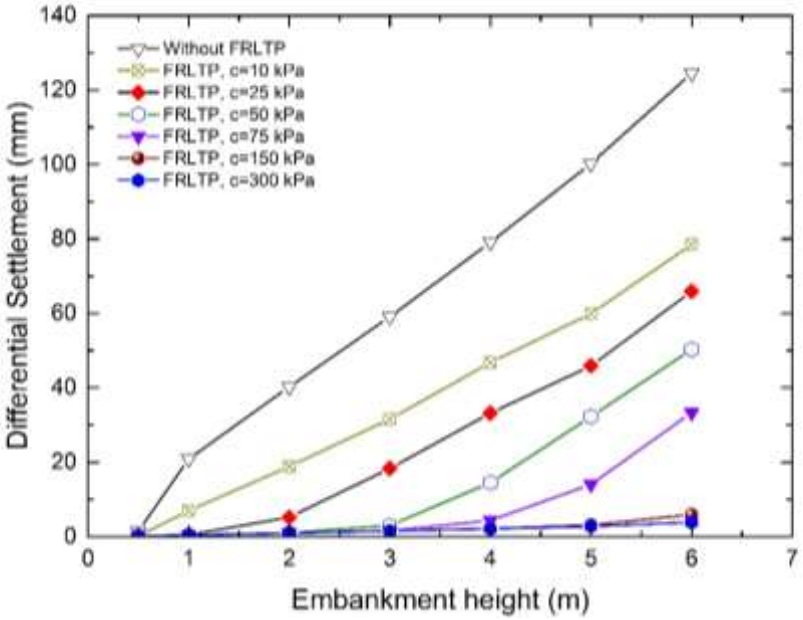

Figure 14 Effect of the FRLTP cohesion on differential settlement

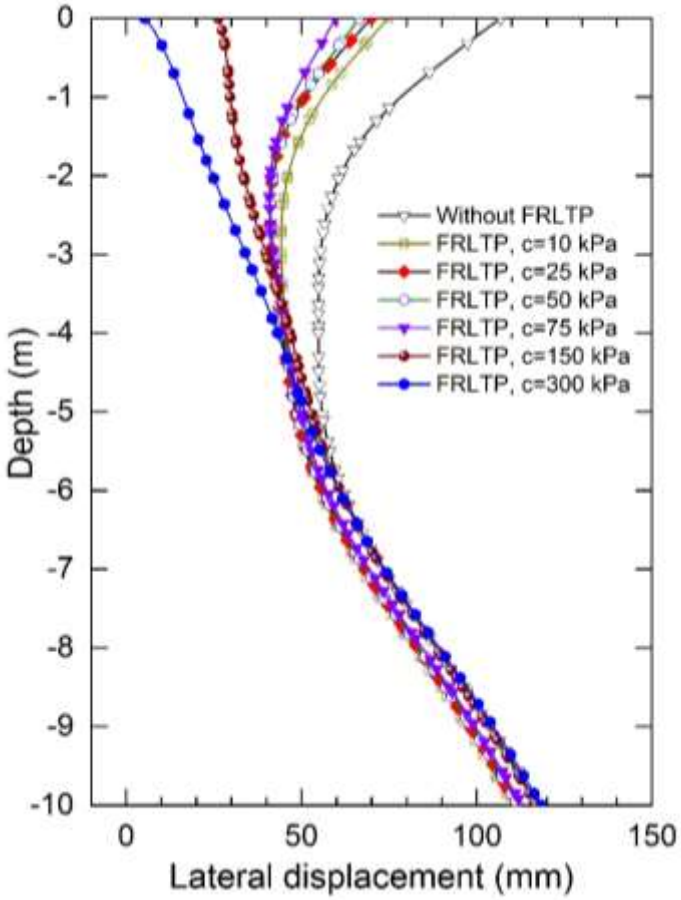

Figure 15 Variation of the lateral displacement with depth for various cohesion values of FRLTP at 2 years post-construction

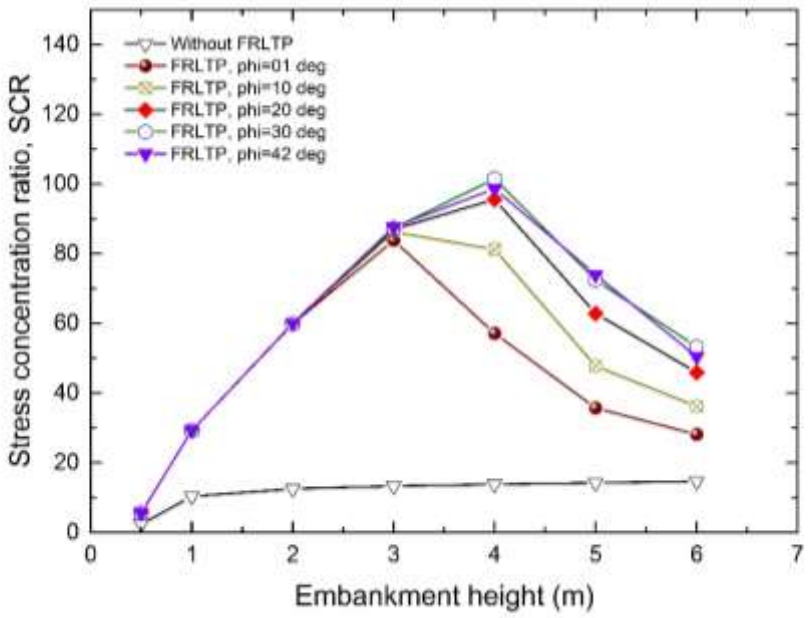

Figure 16 Effect of the FRLTP friction angle on the stress concentration ratio (SCR)

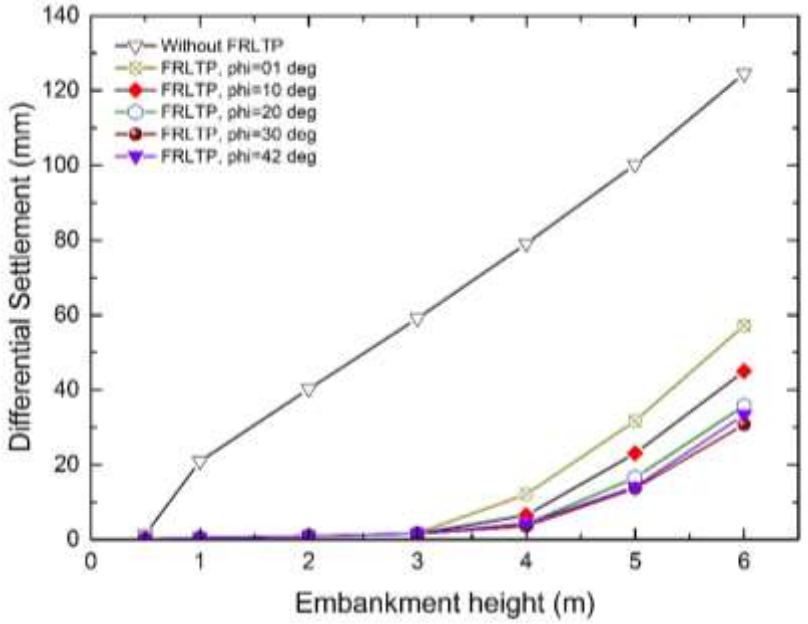

Figure 17 Effect of the FRLTP friction angle on differential settlement

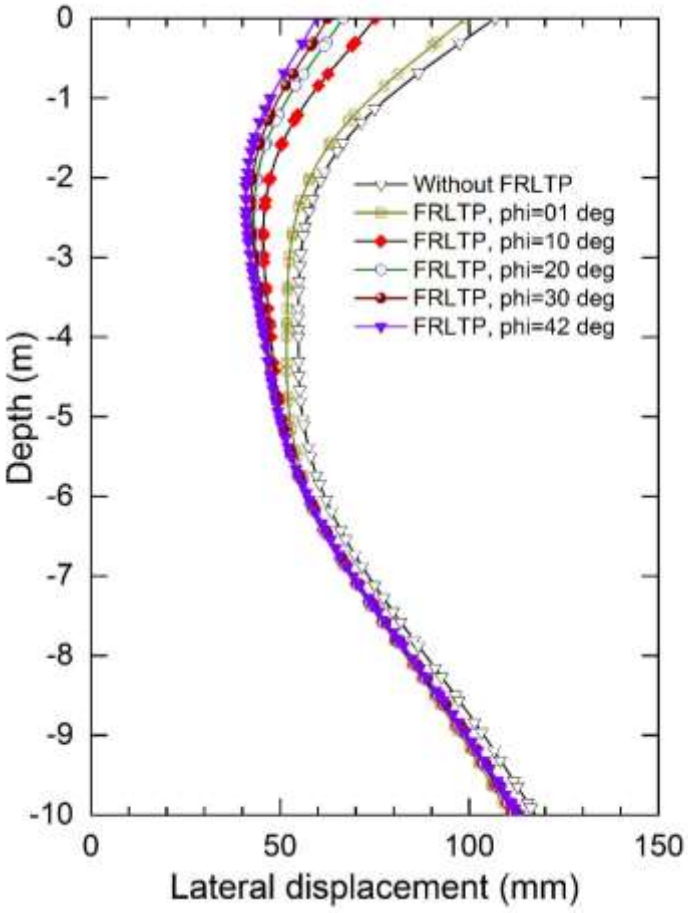

Figure 18 Variation of the lateral displacement with depth for various friction angles of FRLTP at 2 years of post-construction

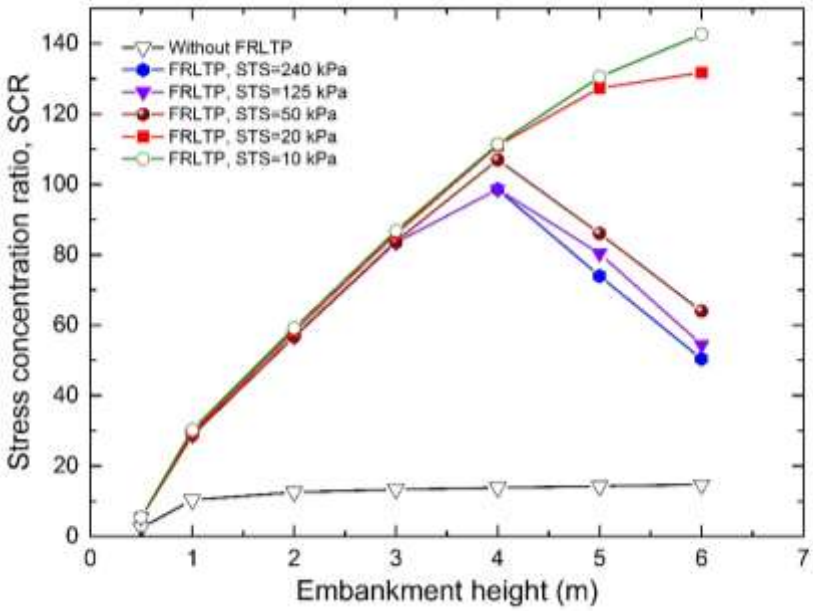

Figure 19 Effect of the FRLTP tensile strength (STS) on stress concentration ratio (SCR)

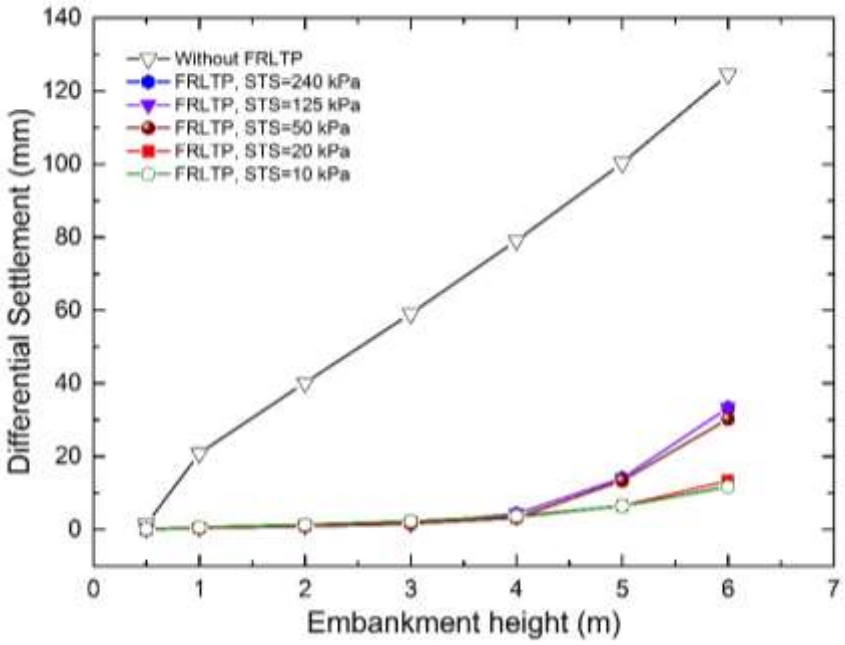

Figure 20 Effect of the FRLTP tensile strength (STS) on differential settlement

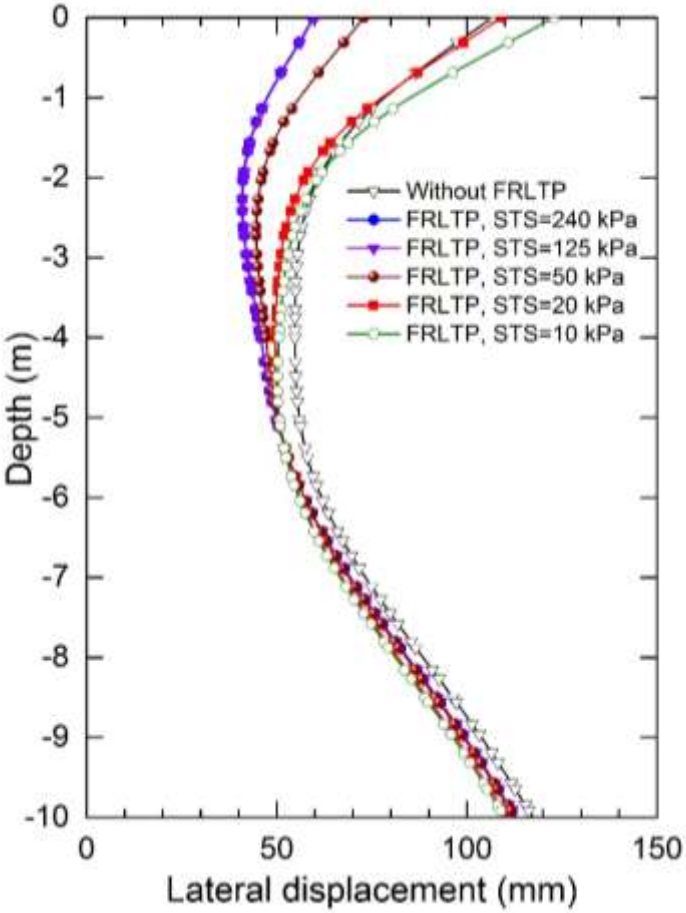

Figure 21 Variation of lateral displacement with depth for various FRLTP tensile strength (STS) at 2 years of post-construction